nagra
National Cooperative for the
Disposal of Radioactive Waste

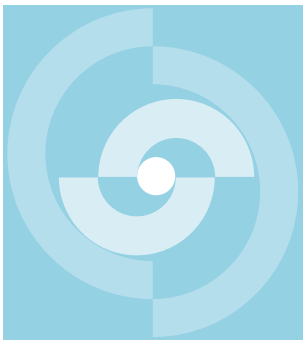

TECHNICAL REPORT 02-13

Redox Conditions in the Near Field of a Repository for SF/HLW and ILW in Opalinus Clay

March 2003

P. Wersin, L.H. Johnson, B. Schwyn
U. Berner, E. Curti

Hardstrasse 73, CH-5430 Wettingen/Switzerland, Telephone +41-56-437 11 11

nagra
National Cooperative for the
Disposal of Radioactive Waste

TECHNICAL REPORT 02-13

Redox Conditions in the Near Field of a Repository for SF/HLW and ILW in Opalinus Clay

March 2003

P. Wersin [1)], L.H. Johnson [1)], B. Schwyn [1)]
U. Berner [2)], E. Curti [2)]

[1)] Nagra, Switzerland

[2)] Paul Scherrer Institut, Villigen PSI, Switzerland

Hardstrasse 73, CH-5430 Wettingen/Switzerland, Telephone +41-56-437 11 11

ISSN 1015-2636

Abstract

The description of redox conditions in the near field of a nuclear waste repository is an important but difficult aspect in performance assessment. Redox potentials are affected by both the thermodynamics and kinetics of relevant reactions, some of which are not adequately understood. This leads to considerable uncertainty of redox conditions in the repository environment and often to oversimplified terminology in performance assessment such as 'reducing' or 'oxidising'. In this study we assess redox conditions by a holistic approach that considers all relevant sources of information. We apply this approach to the near field of the two types of repositories foreseen in the Swiss high-level waste programme: the spent fuel and high-level waste (SF/HLW) and the intermediate-level waste (ILW) repositories. Although the environments surrounding these two waste streams are quite different, namely bentonite backfill versus cement, the procedures for describing redox conditions are similar. Thus, for both cases we first describe the layout of the repository and the properties of materials present in the near field. Then the duration of the initial oxic phase is estimated with the aid of limiting cases. The major part of this study focuses on the thermodynamic relationships and kinetic processes in the engineered barrier once oxygen has been depleted. Finally, from the combined set of information, reasonable ranges of long-term redox potentials are derived.

SF/HLW

After a relatively short initial oxic phase (< 100 a) the conditions in the bentonite backfill will become and remain reducing. The redox potentials will be largely influenced by the corrosion of steel, which will produce large amounts of magnetite, on the internal side of the bentonite barrier, and by the reducing conditions of the surrounding Opalinus Clay on the external side.

The derived Eh range of -100 mV to -300 mV (SHE) for the anoxic stage mainly reflects the relatively large uncertainties in the pH of the porewater. The calculations suggest that the uncertainty with regard to the nature of the Fe(III)-Fe(II) solid phases is less significant in determining the derived redox potentials. The calculated redox potentials are consistent with recent experimental data on the reduction behaviour of U(VI), Tc(VII) and Se(VI/IV).

The possible effect of high hydrogen pressures on redox potentials was not included in the analysis because the experimental data on the reactivity of $H_2(g)$ in bentonite are limited. This also holds for Fe(II)-rich silicate phases which may play a role at the canister - bentonite boundary, although significant effects on the redox potentials are not expected. Further experimental data on these systems would be useful for future performance assessments.

ILW

Heterogeneous reprocessed waste embedded in a cementitious matrix is grouped into two spatially separated waste types, ILW-1 and ILW-2. These two types consist of very different redox-sensitive materials and are assessed separately.

After relatively rapid depletion of residual oxygen the conditions in the ILW-1 repository will remain reducing. The redox potential will be largely influenced by steel corrosion producing thin magnetite-type films on steel surfaces. Based on Fe(III)/Fe(II) equilibria calculations, the derived redox potentials for the reducing stage are estimated to be between -750 and -230 mV (SHE). The redox conditions in ILW-2 are expected to be rather similar; however, they might be more oxidising if high nitrate concentrations persist over long time periods. In this case an upper Eh limit of +350 mV (SHE) is estimated.

The uncertainties with regard to the redox potentials in solution are large, mainly because of the lack of unequivocal experimental information on the phases forming during long-term corrosion of steels and the limited knowledge on iron-bearing cement phases. In addition, the importance of microbially-induced organic matter degradation, though considered to be of minor importance, is not adequately understood. If significant degradation occurs, lower redox potentials would be expected. This would also be the case if H_2 produced by the corrosion process were more reactive than commonly assumed.

Further experimental work focussing on the steel corrosion under alkaline conditions and the identification of iron-bearing phases in the cement repository is needed to improve the understanding of the relevant redox processes. Also, the behaviour of redox- sensitive elements, such as U, Tc and Np in cementitious environments should be experimentally investigated.

Zusammenfassung

Die sachgemässe Darstellung der Redoxbedingungen im Nahfeld eines radioaktiven Lagers ist ein heikler, aber zugleich auch sehr wichtiger Aspekt in der Sicherheitsanalyse. Die massgebenden Redoxpotentiale werden durch thermodynamische und kinetische Eigenschaften von teilweise noch wenig verstandenen Reaktionen beeinflusst. Daraus ergibt sich eine beträchtliche Unsicherheit bezüglich der effektiven Redoxpotentiale im Umfeld des Lagers, was in der Sicherheitsanalyse wiederum zu eher simplistischen Charakterisierungen wie "reduzierend" oder "oxidierend" geführt hat. Die vorliegende Arbeit verwendet zur Beschreibung der Redoxbedingungen einen ganzheitlichen Ansatz, der alle relevanten Informationen berücksichtigt. Wir wenden diesen Ansatz auf das Nahfeld beider im schweizerischen Hochaktivprogramm vorgesehenen Lagertypen an, nämlich das Lager für abgebrannte Brennelemente und hochaktive Abfälle (BE/HAA) und das Lager für langlebige mittelaktive Abfälle (LMA). Obwohl das chemische Umfeld dieser zwei Abfallkategorien ziemlich unterschiedlich ist, auf der einen Seite Bentonit, auf der anderen Seite Zement, werden zur Beschreibung der Redoxbedingungen sehr ähnliche Vorgehensweisen gewählt. Wir beschreiben in beiden Fällen zuerst das Layout des Lagers und die Materialeigenschaften im Nahfeld. Dann schätzen wir die Dauer der oxischen Phase anhand limitierender Fällen ab. Ein wesentlicher Teil der Arbeit konzentriert sich anschliessend auf die Diskussion der Thermodynamik und der kinetischen Prozesse in der technischen Barriere während der anoxischen Phase, d.h. wenn der freie Sauerstoff aufgebraucht ist. Schliesslich werden aus den kombinierten Datensätzen realistische Redoxpotentiale und ihre Unsicherheiten abgeleitet.

BE/HAA

Nach einer relativ kurzen oxischen Phase (<100 Jahre) werden die Bedingungen in der Bentonitverfüllung dauerhaft reduzierend sein. Die Korrosion des Stahls produziert grosse Mengen an Magnetit und beeinflusst die Redoxbedingungen auf der inneren Seite der Bentonitbarriere. Auf der äusseren Seite der Bentonitbarriere werden die Redoxbedingungen vor allem durch den umgebenden Opalinuston beeinflusst.

Der für die anoxische Phase zwischen -100 und -300 mV (NWE) berechnete Eh-Bereich widerspiegelt im wesentlichen die grossen Unsicherheiten bezüglich dem pH des Porenwassers. Die Berechnungen deuten darauf hin, dass die Abweichungen aufgrund der Unsicherheiten in den Fe(III)-Fe(II)-Phasen weniger gross sind. Die abgeleiteten Redoxpotentiale stehen mit neueren experimentellen Daten über das Reduktionsverhalten von U(VI), Tc(VII) und Se(VI/IV) im Einklang. Den möglichen Effekt hoher Wasserstoffdrücke auf Redoxpotentiale haben wir nicht in unsere Analyse mit einbezogen, weil über die Reaktivität von H_2 im Bentonit nur sehr unvollständige Daten vorliegen. Aus ähnlichen Gründen wurden auch die eisenreichen Silikatphasen nicht berücksichtigt. Da deren Einfluss auf das Redoxpotential an der Behälter/Bentonitgrenze als nicht signifikant eingeschätzt wird, ist ein solcher Entscheid nicht kritisch. Die Erhebung weiterer experimenteller Daten zu diesen Systemen wäre für künftige Sicherheitsanalysen sehr hilfreich.

LMA

Diese heterogenen, langlebigen Abfälle aus der Wiederaufbereitung, die in eine Zementmatrix eingeschlossen sind, werden in die räumlich getrennten Typen LMA-1 und LMA-2 aufgeteilt. Die beiden Typen enthalten sehr unterschiedliche, redoxempfindliche Materialien und werden hier separat behandelt.

Nach einer relativ raschen Reduktion des freien Sauerstoffs werden die Bedingungen im LMA-1 reduzierend bleiben. Die Korrosion produziert auf den Stahloberflächen dünne Magnetitfilme, die das Redoxpotential im wesentlichen bestimmen. Basierend auf Fe(III)/Fe(II)-Gleichgewichtsberechnungen werden für die reduzierende Zeitperiode Redoxpotentiale im Bereich von -750 bis -230 mV (NWE) abgeschätzt. Eigentlich würden für den Abfalltyp LMA-2 ähnliche Bedingungen erwartet. Falls jedoch die hohen Nitratkonzentrationen über längere Zeit nicht abgebaut werden, könnten sich oxidierende Bedingungen im Bereich von +350 mV (NWE) einstellen.

Bedingt durch den eingeschränkten Wissensstand zu den durch Langzeitkorrosion oder im Zement gebildeten Eisenphasen ergeben sich grosse Unsicherheiten für das Redoxpotential in der Porenlösung. Die Rolle des mikrobiellen Abbaus von organischem Material kann ebenfalls nicht schlüssig beurteilt werden. Im Falle eines signifikanten Abbaus von organischem Material würden generell tiefere Redoxpotentiale erwartet. Dies wäre auch der Fall, wenn das durch Korrosionsprozesse entstandene H_2 reaktiver wäre als gemeinhin angenommen.

Um für die relevanten Redoxprozesse ein besseres Verständnis zu erreichen, sind weitere experimentelle Arbeiten erforderlich. Diese sollten auf die Stahlkorrosion unter alkalischen Bedingungen und auf die Identifikation von eisenhaltigen Phasen im Zementlagern ausgerichtet sein. Zudem sollte das Verhalten von redoxempfindlichen Elementen wie U, Tc und Np unter Zementbedingungen experimentell untersucht werden.

Résumé

La description des conditions redox dans le champ proche d'un dépôt pour déchets radioactifs est un aspect important, mais problématique, des analyses de sûreté. Les potentiels redox sont subordonnés aux aspects thermodynamiques aussi bien que cinétiques des réactions d'oxydoréduction, dont certaines n'ont pas encore été cernées de manière satisfaisante. Ceci conduit à des incertitudes considérables concernant les conditions redox dans l'environnement du dépôt, et souvent à des simplifications exagérées dans le cadre des analyses de sûreté, aboutissant à qualifier d'une façon générale les conditions d'"oxydantes" ou de "réductrices". La présente étude aborde les conditions redox par le biais d'une approche holistique prenant en compte toutes les sources d'information pertinentes. Cette approche est appliquée au champ proche de deux types de dépôts envisagés dans le cadre du programme suisse de gestion des déchets hautement radioactifs: le dépôt pour assemblages combustibles usés et déchets de haute activité (AC/DHA) et le dépôt pour déchets de moyenne activité à vie longue (DMAL). Bien que ces deux environnements présentent certaines différences (remplissage de bentonite dans un cas, ciment dans l'autre), les procédures qui permettent de décrire les conditions redox sont similaires. Ainsi, dans les deux cas, nous commençons par décrire l'architecture de dépôt et les propriétés des matériaux du champ proche. La durée de la phase oxique initiale est ensuite évaluée à l'aide de cas limites. La majeure partie de cette étude est axée sur les relations thermodynamiques et les processus cinétiques qui se déroulent dans le système de barrières ouvragées une fois que l'oxygène a disparu. Enfin, en combinant toutes les informations obtenues, il est possible de déduire des valeurs réalistes pour les potentiels redox à long terme et les incertitudes qui leur sont liées.

AC/DHA

A l'issue d'une phase oxique initiale relativement courte (< 100 ans), les conditions régnant dans le remplissage de bentonite deviennent réductrices. Sur la face interne de la barrière de bentonite, la corrosion de l'acier, en produisant de grandes quantités de magnétite, aura un impact important sur les potentiels redox. Sur la face externe, c'est le milieu réducteur des Argiles à Opalinus qui sera déterminant.

L'écart important entre les mesures Eh obtenues – de -100 mV à -300 mV (SHE, Standard Hydrogen Electrode) pour la phase anoxique – est dû principalement aux incertitudes qui subsistent quant au pH de l'eau interstitielle. Les calculs effectués suggèrent que l'incertitude relative aux phases de Fe(III)-Fe(II) est moins importante pour la dérivation des potentiels redox. Les potentiels redox calculées sont compatibles avec les données expérimentales récentes concernant la réduction de U(VI), Tc(VII) et Se(VI/IV).

L'impact possible d'une pression d'hydrogène élevée sur les potentiels redox n'a pas été abordé dans le cadre de cette étude, en l'absence de données expérimentales concluantes sur la réactivité de $H_2(g)$ dans la bentonite. Ceci vaut également pour les phases de silicate riches en Fe(II), qui peuvent jouer un rôle à l'interface colis de déchets–bentonite, bien que leur influence sur les potentiels redox soit probablement limitée. Pour les analyses de sûreté à venir, il serait utile de disposer de données expérimentales supplémentaires à ce propos.

DMAL

Les DMAL sont composés de déchets hétérogènes, provenant des opérations de retraitement et immobilisés dans une matrice de ciment. On distingue deux groupes, les DMAL-1 et DMAL-2,

stockés à des emplacements distincts. Ces deux groupes sont analysés séparément du fait qu'ils contiennent des matériaux dont la sensibilité aux processus redox est très différente.

Après la disparition relativement rapide de l'oxygène résiduel, les conditions régnant dans le dépôt DMAL-1 resteront réductrices. Le potentiel redox sera alors principalement influencé par la corrosion de l'acier, qui produit un mince film de magnétite à la surface du métal. Sur la base des calculs d'équilibre sur Fe(III)/Fe(II), les potentiels redox dérivés pour la phase réductrice se situent entre -750 et -230 mV (SHE). Les conditions redox dans le dépôt DMAL-2 seront probablement assez similaires. Toutefois, si de hautes concentrations de nitrates subsistaient sur de longues périodes, il est possible que les valeurs Eh atteignent +350 mV (SHE).

Il subsiste d'importantes incertitudes relatives aux potentiels redox dans l'eau interstitielle, dues principalement à l'absence de données expérimentales solides sur la formation de phases au cours de la corrosion de l'acier sur de longues périodes, et à des connaissances insuffisantes sur les phases du ciment riches en fer. De plus, on manque de données précises sur la dégradation microbienne des matières organiques; toutefois, on suppose que celle-ci aurait un impact réduit. En présence d'une dégradation importante de matières organiques, on peut s'attendre d'une manière générale à des potentiels redox plus bas, ce qui serait également le cas si l'hydrogène produit par le processus de corrosion s'avérait plus réactif qu'on ne le suppose habituellement.

Afin de mieux appréhender les processus redox, il serait nécessaire de disposer de données expérimentales supplémentaires concernant la corrosion de l'acier dans des conditions alcalines et l'identification des phases riches en fer dans un dépôt contenant du ciment. De même, il serait utile d'effectuer des expériences sur le comportement de radioéléments sensibles aux processus redox, tels que U, Tc et Np, dans un environnement comportant du ciment.

Table of Contents

Abstract I
Zusammenfassung III
Résumé V
Table of Contents VII
List of Figures IX
List of Tables IX
Introduction 1

PART A - SPENT FUEL & HIGH-LEVEL WASTE (SF/HLW) 3
1 Properties of Materials Present in the Near Field Relevant to Redox Evolution 3
2 General concept of redox evolution 4
2.1 General aspects 4
2.2 Microbial processes 5
2.3 Time scales for oxygen depletion 5
3 Which phases control redox conditions? 7
3.1 Iron phases 7
3.2 Other phases 9
3.3 Opalinus Clay host rock 9
4 Indications from radionuclide reactions 11
5 Derivation of redox potentials 12
5.1 Rationale 12
5.2 Thermodynamic modelling 13
5.2.1 Bases for modelling 13
5.2.2 Results 15
5.2.3 Discussion 16
5.3 Kinetics 17
6 Conclusions for the SF/HLW case 17

PART B - INTERMEDIATE-LEVEL WASTE (ILW) 19
7 General concept of redox evolution 19
7.1 Waste inventory and redox-sensitive compounds 19
7.2 Oxic stage 21
7.3 Anoxic stage 22

8 Discussion of different redox processes 23
8.1 Anoxic corrosion of steel 23
8.2 Dissolution of fuel waste 23
8.3 Microbially-induced processes 24
8.4 Diffusion of reduced species from the host rock 25
9 Estimation of redox potentials 25
9.1 Bases for model calculations 25
9.1.1 ILW-1 26
9.1.2 ILW-2 26
9.1.3 Porewater compositions 26
9.1.4 Redox control by iron phases 27
9.2 Results for ILW-1 30
9.3 Results for ILW-2 31
10 Conclusions for the ILW case 31
Acknowledgements 32
11 References 32

APPENDIX A - Estimation of time scales for O_2 consumption ..... A-I

List of Figures

Figure 1.0: Layout of the Swiss repository for SF/HLW and ILW waste in the Opalinus Clay host rock. 1

Figure 1.1: Layout and dimensions of the engineered barrier system for a spent fuel emplacement tunnel. 3

Figure 3.1: Schematic picture of major redox-active phases present in engineered barrier and host rock 7

Figure 3.2: Stability field of iron phases in Eh-pH diagram in Fe-CO_2-SO_4-H_2O system. 10

Figure 7.1: Disposal schema for ILW. 20

Figure 9.1: pH-Eh diagram for the Fe-CO_2-H_2O system. 29

Figure A1: Relative oxygen concentration at the bentonite/host rock interface. ..... A-II

Figure A2: Relative oxygen concentration at the O_2 front in the host rock (SF/HLW case) ..... A-IV

List of Tables

Table 5.1: Porewater composition in mol/L for the bentonite backfill as derived by CURTI and WERSIN (2002) 14

Table 5.2: Iron equilibria and logK constants (taken from HUMMEL et al. 2002) used for thermodynamic calculations 14

Table 5.3: Derived redox potentials in near field of SF/HLW. Various Fe(III)/Fe(II) equilibria assumed (SI = saturation index). 16

Table 7.1: Redox inventory of ILW-1 and ILW-2 (calculated from SCHWYN et al. 2003) 21

Table 9.1: Porewater composition for ILW-1 and ILW-2 27

Table 9.2: Solid iron phase equilibria used for thermodynamic calculations. 28

Table 9.3: Test runs for different Fe(III)/Fe(II) equilibria for ILW-1. 30

Introduction

The Swiss concept for the disposal of high-level waste foresees a repository for two different waste types (NAGRA 2002a). The first waste type includes both spent fuel and reprocessed vitrified high-level waste (SF/HLW) contained in steel canisters and surrounded by bentonite backfill. The second waste type, located at least 500 m away from the SF/HLW, includes various intermediate-level waste (ILW) streams derived from reprocessing. Most of these wastes will be incorporated in a cementitious matrix, a small part will be incorporated in bitumen. The layout of the repository is shown in Figure 1.0. The near fields of the SF/HLW (canister-bentonite) and ILW (cement) display distinct geochemical environments. However, they share a number of common features in terms of redox properties, as is pointed out below.

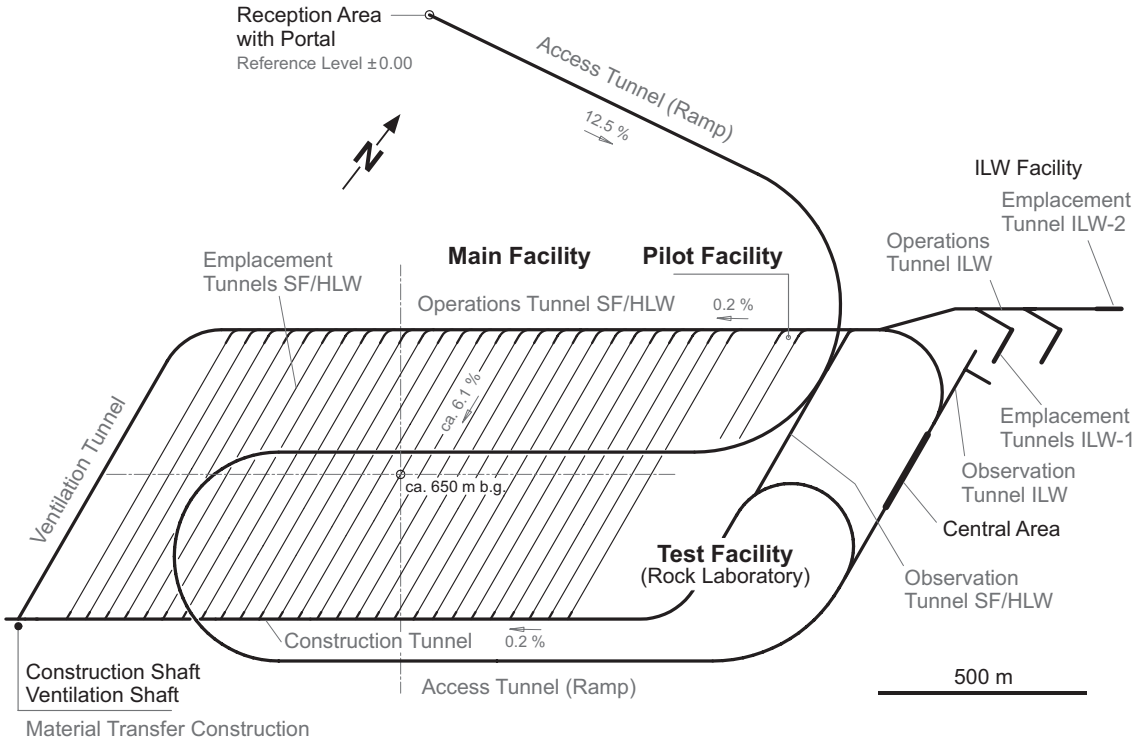

Figure 1.0: Layout of the Swiss repository for SF/HLW and ILW waste in the Opalinus Clay host rock.

The determination of redox conditions in the near field of a repository constitutes an important aspect of safety assessment. Redox conditions strongly affect the mobility and sorption of many radionuclides such as uranium, neptunium, plutonium, technetium and selenium. These elements are highly relevant in the safety assessment of the SF/HLW and ILW repository. In order to predict the fate of redox-sensitive radionuclides, the redox potential (Eh) in the near-field porewater needs to be estimated. Factors which may affect redox conditions in the porewater include:

1. the type and corrosion rate of steel (e.g., canisters, reinforcement in concrete),

2. the quantity of oxygen entrapped in the engineered barriers (bentonite, mortar/concrete),

3. the types of redox-active minerals present in the engineered barriers and in the surrounding rock,

4. the presence and viability of microbes, which are important catalysts in many redox reactions,

5. the rate of diffusion of redox-sensitive species from the rock, and

6. the production of radiolytic oxidants and reductants from spent fuel or compacted hulls in the ILW.

Moreover, in the case of SF/HLW, the rates of redox processes may be influenced significantly by elevated temperatures, which are expected to exceed 100°C close to the canisters and reach a maximum of ~60°C in the surrounding rock (JOHNSON et al. 2002). With these considerations in mind, it is evident that redox conditions cannot be simply determined through a single chemical equilibrium model, where all redox couples are simultaneously at equilibrium. The determination of redox conditions requires a holistic approach which considers all relevant sources of information, also including the kinetics and reactivity of the redox-active species involved.

The main objectives of this work are:

- to provide the thermodynamic and kinetic framework for the near field of the SF/HLW and ILW repositories,
- to constrain the redox potentials relevant at long time scales and estimate uncertainties thereof, as a basis for predicting solubilities and sorption of redox-sensitive radionuclides.

The approaches used for assessing redox conditions in the canister-bentonite and cementitous environment are similar. We first describe the layout of the repository and the properties of materials present in the near field. Then the duration of the initial oxic phase is estimated with the aid of limiting cases. The major part focuses on redox processes in the near field once oxygen has been depleted. The importance of the different redox-active phases for influencing redox potentials is discussed. Moreover, recent work on the reduction behaviour of redox-sensitive radioelements (e.g., U, Tc, Np, Se) at near-field like conditions is presented. From this combined set of information the complex redox system is simplified within a thermodynamic framework that assumes redox control by Fe(III)/Fe(II) reactions (e.g. JOBE et al. 1997). Finally, redox potentials for the porewaters in the bentonite backfill and cement are derived and uncertainties thereof estimated.

The assessment of redox conditions is presented separately for SF/HLW and ILW in Parts A and B respectively. This introduces some redundancy, but, in our view, adds to the clarity of the report. It should be noted in this respect that the waste streams in ILW are much more heterogeneous than the ones of SF/HLW.

PART A - SPENT FUEL & HIGH-LEVEL WASTE (SF/HLW)

1 Properties of Materials Present in the Near Field Relevant to Redox Evolution

The layout of a disposal tunnel for the spent fuel repository is shown in Figure 1.1. The cast steel canisters rest on blocks of highly compacted bentonite, with the remaining volume filled with granular bentonite. The average dry density of the bentonite surrounding the canisters is 1.5 Mg m^{-3}, thus its initial porosity is ~0.45. Upon emplacement, the bentonite is expected to have a moisture content of ~2%. This means that only ~5% of the voids in the bentonite are filled with water. Based on a volume of bentonite per canister of ~35 m^3, the bentonite will contain ~123 moles of oxygen gas. The surrounding Opalinus Clay has a porosity of ~0.12. Under normal conditions, the pores will be saturated; however, excavation of the tunnels and operation of a ventilation system will tend to partially desaturate a region of surrounding rock, referred to as the excavation disturbed zone (EDZ). Here we assume that the EDZ is ~0.5 m thick (NAGRA 2002a) , and that drying reduces its moisture content by ~50%. This implies that the EDZ might contain a further 23 moles of oxygen per canister.

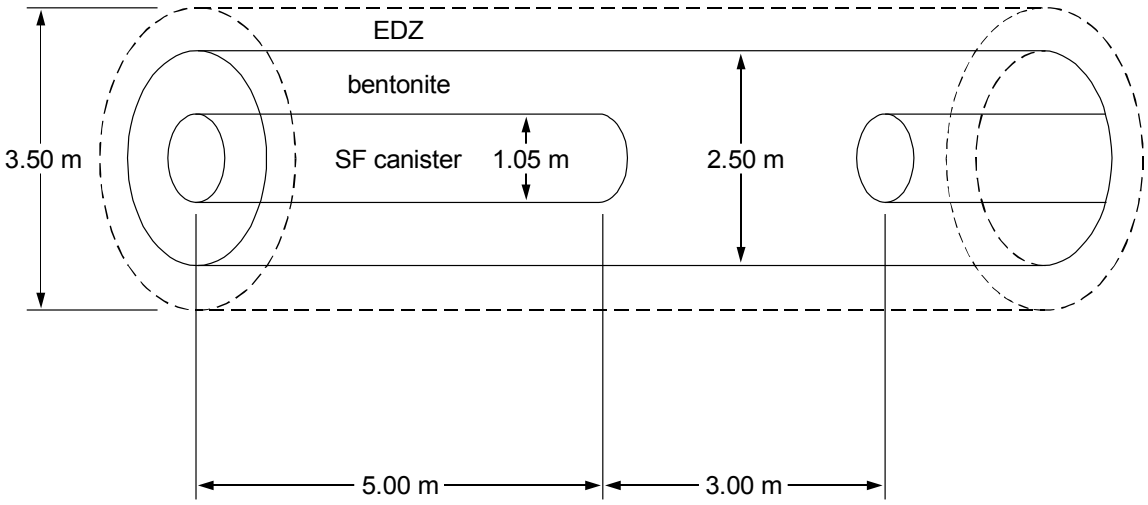

Figure 1.1: Layout and dimensions of the engineered barrier system for a spent fuel emplacement tunnel.

The bentonite is expected to contain some redox-active minerals. For example, MÜLLER-VONMOOS & KAHR (1983) reported that MX-80 bentonite contains 0.7 wt% siderite ($FeCO_3$) and 0.3 wt% pyrite (FeS_2). In addition, traces of iron oxides may be present (BAEYENS & BRADBURY 1995). Because there is uncertainty about what type of bentonite would be used in the repository and because there is variability in bentonite composition, caution must be used when considering the role of these materials in redox reactions in the near field. Furthermore, the montmorillonite fraction in MX-80 typically contains structural iron of 2 wt%, most of which is Fe(III) (VOGT & KÖSTER 1978).

The Opalinus Clay contains a rather large portion of Fe(II) minerals. Thus, pyrite concentrations show a range of 0.2 - 1.4% and an average of about 1% (MÄDER & MAZUREK 1998; NAGRA 2002b). In addition, siderite (4 ± 2.4%) and traces of ankerite are detected (NAGRA 2002b).

The SF and HLW canisters are assumed to be fabricated from carbon steel or cast iron. The canister masses are, depending on the canister type, between 21 and 26 t. This amounts to approximately 400 kmol of elemental Fe per canister. The gamma radiation field from a spent fuel or HLW canister is relatively low (<35 mGy hr^{-1}). MARSH & TAYLOR (1988) studied corrosion of carbon steel as a function of radiation dose rate, and observed negligible increases in corrosion rates below 3'000 mGy hr^{-1}, thus gamma radiation is not expected to enhance corrosion.

2 General concept of redox evolution

2.1 General aspects

It is useful to distinguish two phases in the evolution of redox conditions in the near field:

(1) Before canister failure

In an initial stage, the residual oxygen entrapped in the pores of the bentonite and in the EDZ may react with reduced phases in the bentonite and in the EDZ, as well as with the steel canister (NERETNIEKS 1983; WERSIN et al. 1994a). The relative rates of these processes are strongly dependent on the degree of water saturation of the near field, which itself is influenced by temperature and by the hydraulic conductivity of the surrounding rock. After consumption of oxygen, conditions in the bentonite will be reducing. The corresponding redox potentials will be affected by the anoxic corrosion of steel, which will produce mainly magnetite and H_2, and by diffusion of redox-active species from the reduced host rock. The microbially-mediated process of sulphate reduction will most likely be inhibited because bacterial activity in bentonite systems is restricted to low densities (dry densities < 1.2 Mg m^{-3}; PUSCH 1999).

In Section 2.2 the time scales for consumption of oxygen are evaluated, based on different assumptions regarding the time over which bentonite saturation would occur.

(2) After canister failure

Corrosion of steel will extend to the inner parts of the canister and increase the amounts of corrosion products. Spent fuel dissolution will begin, influenced by radiolysis of water which will produce oxidised species and H_2. The impact of this process is still under debate. Recent experiments (RÖLLIN et al. 2001, KING et al. 1999) suggest that the fuel dissolution rate is strongly reduced at high pressures of H_2 at radiation dose rates typical of spent fuel. The effect of the released radiolytic oxidants on redox conditions in the near field was assessed in a coupled mass balance model by JOHNSON & SMITH (2000). Their results indicate that, under pessimistic assumptions (H_2 is non-reactive and passivation of magnetite limits the release of Fe(II) to solution), the canister environment could become oxidising, but the largest part of the bentonite would remain reducing. The redox conditions in the reduced part are not expected to differ significantly from those established just before canister failure. As noted, this model implicitly assumes that H_2 is chemically inert under these conditions.

2.2 Microbial processes

Microbial processes play a major role in the transformation of redox-sensitive elements in aquatic systems and thus may be important for many performance assessment aspects (WEST et al. 2002; PEDERSEN 2000). For example, microbially mediated iron, sulphate and even CO_2 reduction may occur in deep geological environments, such as granitic rocks (PEDERSEN 1997).

The Redox Experiment in Detailed Scale (REX) at the Äspö Hard Rock Laboratory in which the reactivity of O_2 trapped in a closed repository was studied, revealed the importance of microbes as catalysts (PUIGDOMENECH et al. 2001). In fact, results indicate the substantial contribution of microbial activity to the rate of O_2 uptake, leading to rapid O_2 depletion within a few days.

Relatively few studies have looked at microbial effects in engineered barrier systems such as compacted bentonite (GLAUS 2001). Experimental data with sulphate-reducing bacteria in bentonite indicate that there is no bacterial activity above densities of 1.5 Mg m^{-3} (PEDERSEN et al. 2000). The large scale experiment (LOT) performed in the Äspö Hard Rock Laboratory included the introduction of a large number of microorganisms in the bentonite backfill materials. The results after 72 hours indicate the elimination of all bacteria but the spore-forming species which, however, are metabolically inactive and show a slow but significant death rate. These considerations and further experimental and theoretical evidence suggest that bacterial viability in compacted bentonite is very unlikely because of the low porosities and the reduced water activity (STROES-GASCOYNE & WEST 1997; PUSCH 1999; STROES-GASCOYNE 2002).

The role of microbial effects in Opalinus Clay is at present unclear, although this environment is also expected to be very hostile for bacteria, such as sulphate reducers (STROES-GASCOYNE 2002). However, because of the long residence time of porewater (i.e. millions of years) sulphate reduction may have occurred (PEARSON 2002).

2.3 Time scales for oxygen depletion

Water inflow rates to the near field are expected to be very slow, as a result of the low hydraulic conductivity of Opalinus Clay. For example, for an estimated hydraulic conductivity of Opalinus Clay of 10^{-13} m s^{-1} (NAGRA 2002b) the time for saturation of the bentonite surrounding the canister ranges from ~100 a to many hundreds of years. Although reactions involving oxygen will proceed well before full saturation, they are likely to be very much retarded during the very early stages of repository evolution when the moisture content of the bentonite is close to its initial 2% value. Furthermore, the high temperatures at the canister surface, which will be above 100°C for long time periods (>100 a) (JOHNSON et al. 2002), will maintain a low moisture content in this region for a considerable time (see, for example, BÖRGESSON & HERNELIND 1999). This will strongly decrease canister corrosion rates. For example, studies of steel corrosion show that, in air, corrosion of mild steel or cast iron is extremely slow below the critical relative humidity of ~60% (BROWN & MASTERS 1982). In contact with bentonite, the critical relative humidity for initiation of aqueous corrosion may be reduced to about 30% due to absorption of water by hygroscopic salts, in particular, trace quantities of $CaCl_2$ or NaCl present in bentonite, and by capillary condensation (MANSFELD & KENKEL 1976, KUCERA & MATTSON 1987). Nonetheless, a relative humidity of 30% is still well above the range initially expected near the canister surface. Because the initial steel corrosion by oxygen will most likely be initially very slow, other materials may consume the oxygen. One such possibility is the oxidation of pyrite and other Fe(II)-bearing minerals within the excavated damaged zone (EDZ), where moisture levels will be considerably higher than in

the bentonite, and thus able to support the alteration of these minerals. The high diffusivity of oxygen in unsaturated bentonite would permit the oxygen to diffuse rapidly to this region as it is consumed.

Because there are considerable uncertainties associated with the above discussion, we consider it useful to evaluate the rates of three different cases that represent both realistic and extreme scenarios for oxygen consumption in the near field. These are as follows:

Case 1 - Partially saturated conditions with uniform corrosion

The bentonite is partially saturated, with the degree of saturation high enough to sustain uniform corrosion (i.e., greater than ~30% relative humidity, as discussed above). This is considered to be a scenario unlikely to occur within the first few decades after repository closure, because of slow water inflow rates. The time for oxygen consumption for this case is estimated according to the procedure given in Appendix A. Since diffusion is fast in unsaturated bentonite the rate of consumption can be directly related to the corrosion rate of steel. The obtained time of oxygen consumption is about 4 years.

Case 2 - Fully saturated bentonite with uniform corrosion

This is an unrealistic but illustrative case. Under these conditions diffusion is slow, hence it can be inferred that the rate of oxygen consumption by canister corrosion is transport limited. From the solution to the diffusion equation (cf. Appendix A) it is deduced that the time for oxygen consumption at the outer edge of the bentonite is about 50 years.

Case 3 - Negligible canister corrosion with O_2 reacting with pyrite in the EDZ

The moisture content of the bentonite is too low to sustain canister corrosion. Oxygen will rapidly diffuse out into the EDZ and react in the unoxidised host rock. Since pyrite oxidation is fast relative to diffusion in the rock, O_2 consumption is transport limited. Oxygen depletion is strongly dependent on the diffusion coefficient and the pyrite concentration in the rock. The treatment for estimating the time scales under the assumption of steady-state diffusion is given in Appendix A. Because of uncertainties involved in the reactive pyrite surface area and the diffusion coefficient in the EDZ two bounding cases reflecting a realistic and a pessimistic case are considered. The derived time for oxygen depletion (with $C/C_0 = 0.01$) are 2 and 100 years respectively.

The results of the three cases indicate that the flux of oxygen depends on a number of variables and boundary conditions, some of which are not well known. Nevertheless, it can be inferred that oxygen consumption after closure of the repository will occur within less than 100 years. This time will be strongly decreased if unsaturated conditions in the EDZ prevail. It is noteworthy that if there are sufficient reductants in the bentonite the time will also be considerably shorter. Shorter oxygen consumption rates are also expected in the case of microbially-mediated reactions in the host rock (e.g., PUIGDOMENECH et al. 2001). However, because their role at present is uncertain, we have not included them in our considerations.

3 Which phases control redox conditions?

After the initial depletion of oxygen there are a number of redox-sensitive phases and aqueous species which could potentially influence redox conditions. There is general agreement that the selection of appropriate redox equilibria is difficult in the near-field environment in which many thermodynamic equilibria may be relevant, but kinetic control of redox reactions may be the most important consideration. In this context it is important to consider the spatial distribution of the redox-sensitive phases at long time scales, as schematically illustrated in Fig. 3.1. The canister consists of large amounts of iron and corrosion products (magnetite and possibly green rust - GR). The bentonite backfill will have a far lower reducing capacity, since only traces of reactive iron minerals, such as siderite, pyrite and iron oxides (section 2) are present. However, at the other side of the barrier the Opalinus Clay displays a much higher reducing capacity because of its substantial contents of siderite and pyrite. This suggests that the redox conditions in the near field will be different, depending on the location. On the other hand, since at both sides very reducing conditions will prevail, it is not conceivable that significantly more oxidising conditions should occur within the bentonite backfill.

The importance of the different phases affecting the redox conditions is discussed in the following sections.

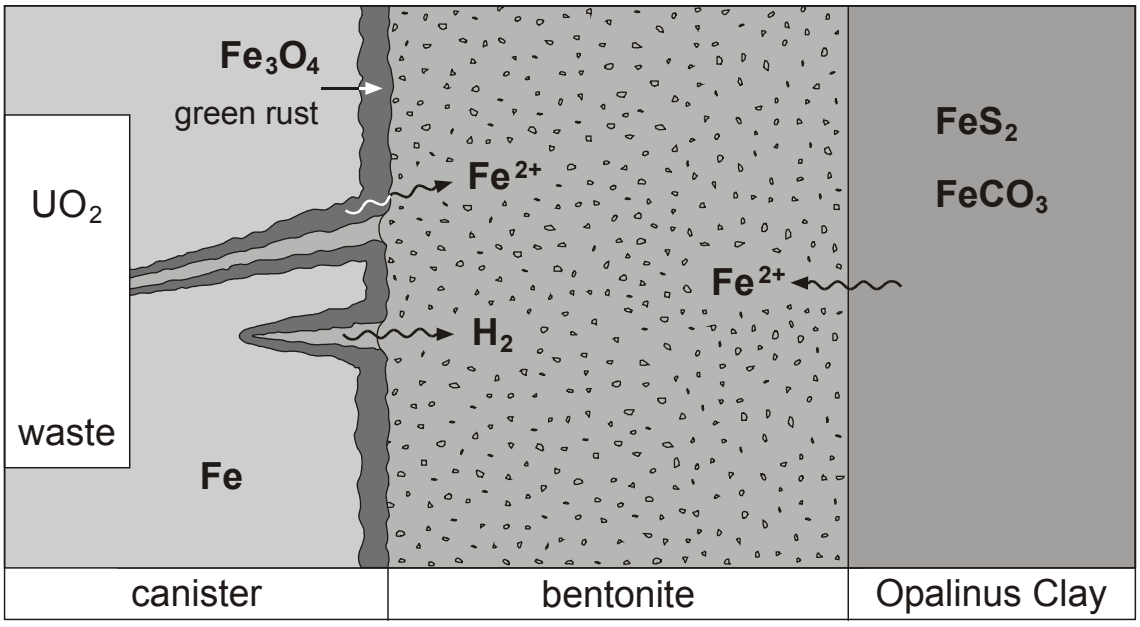

Figure 3.1: Schematic picture of major redox-active phases present in engineered barrier and host rock

3.1 Iron phases

Because of the massive amounts of iron (steel, corrosion products, impurities in bentonite) and the ease of electron transfer between Fe^{3+} and Fe^{2+} relative to other redox couples, it is usually assumed that iron phases control redox conditions in the near field (JOBE et al. 1997; KING & STROES-GASCOYNE 2000).

Magnetite: The formation of Fe_3O_4 during the anoxic corrosion of the steel canister is well established (e.g., SIMPSON 1984; KREIS 1991). Under these conditions, Fe(III) oxides that may have formed in the initial oxidising environment or occurring as impurities in the backfill material, will react with Fe(II) and also lead to magnetite formation (ISHIKAWA et al. 1998). It is thus reasonable to assume that magnetite, which will be present in large quantities, will exert a strong influence on redox conditions. Due to galvanic coupling of magnetite and elemental Fe the redox potential close to the canister surface will be very low (KING & STROES-GASCOYNE 2000). Farther away from the canister spalled-off magnetite (JOHNSON & SMITH 2000) may affect redox conditions.

Siderite: $FeCO_3$ may be present as an impurity in MX-80 bentonite (MÜLLER-VONMOOS & KAHR 1983) and constitutes an important compound in Opalinus Clay (NAGRA 2002b). The solubility of siderite is relatively high ([Fe] = 10 - 100 μM) for the expected porewater compositions. As presented in chapter 6, thermodynamic modelling suggests that bentonite porewater is rather close to equilibrium with regard to siderite.

Pyrite: Pyrite may be present as an impurity in MX-80 (MÜLLER-VONMOOS 1983). Furthermore, pyrite is a prominent mineral phase in the surrounding Opalinus Clay. Pearson (2002) assumed that porewater in the host rock is in equilibrium with pyrite although there is no clear evidence for this assumption. Accepting the assumption that no microbially-mediated sulphate reduction will take place in the compacted bentonite, significant transformation reactions involving pyrite (or FeS) will not occur in the anoxic stage. On the other hand, partial dissolution of pre-existing pyrite is likely to occur during the initial oxic stage.

Fe(III) oxides: Fe oxides may be present as traces (BAEYENS & BRADBURY 1995) in MX-80 or as corrosion products formed during the transitory oxic stage. Under anoxic conditions they will, in the presence of dissolved Fe(II), transform to magnetite (ISHIKAWA et al. 1998). The transformation rate strongly depends on the nature of the iron oxide. Their persistence increases with increasing crystallinity and stability of the iron oxide (KING & STROES-GASCOYNE 2000). Thus, the transformation rate will be relatively fast for amorphous and poorly crystalline phases, such as akaganeite (β-FeOOH), but very slow for hematite (α-Fe_2O_3).

Green rust: Poorly crystalline Fe(III)-Fe(II) hydroxides, termed green rust (GR), are often formed as corrosion products of iron or steel surfaces under reducing conditions (ABDELMOULA et al. 1996; NOVAKOVA et al. 1997). Depending on the solution composition they may incorporate varying amounts of Cl^-, SO_4^{2-} or CO_3^{2-}. Based on electrode potential measurements, thermodynamic properties of GR have been estimated (DRISSI et al. 1995; GÉNIN et al. 1998). These suggest that in most geochemical environments GR is thermodynamically metastable relative to magnetite and siderite. However, recent data suggest that the formation of GR may play an important role in iron-cycling in soils (GÉNIN et al. 1998) and also in the steel corrosion process under repository-like conditions (CUI & SPAHIU 2002).

Iron silicates: In the vicinity of the corroded canister dissolved Fe(II) may react with smectites and lead to Fe(II)-rich silicate phases, such as nontronite or berthierine (GRAUER 1990). The thermodynamic properties of these phases are still poorly known, but constitute a field of active research (e.g. MADSEN 1998, GUILLAUME et al. 2001). The structural iron in bentonite is generally considered as far less reactive than iron mineral impurities, such as siderite, pyrite or iron oxide. Reduction of structural Fe^{3+} in smectite has been shown to occur in the presence of strong reducing agents, such as dithionite (STUCKI 1988; HELLER-KALLAI 1997), or bacteria (KOSTKA et al. 1999).

It is instructive to consider the thermodynamic relationships and stability fields of the Fe-CO_2-H_2O system under the geochemical conditions expected for the bentonite porewater (section 6). This is done by constructing Eh-pH diagrams, as depicted in Fig. 3.2. Note that in these diagrams iron silicates and GR phases are not considered because of lack of reliable thermodynamic data. Moreover, because of kinetic hindrance of sulphate reduction, sulphide equilibria are not included either. In Fig. 3.2a crystalline goethite is assumed to be the stable ferric oxide. This leads to a large stability field of goethite and restricts that of magnetite to alkaline conditions. The most important point to note, however is, that Fe(III)/Fe(II) equilibria fix the redox potentials to low values. If microcrystalline ferric hydroxide is assumed to persist the picture changes substantially (Fig. 3.2b). The stability field of ferric hydroxide is strongly reduced in favour of magnetite. However, now there are two different Fe(III)/Fe(II) equilibrium ranges: one at reducing potentials controlled by magnetite/siderite and one at oxidising potentials, controlled by magnetite/ferric hyroxide. As is discussed in chapter 5 the latter redox couple is not considered relevant under near-field conditions.

3.2 Other phases

Hydrogen gas: It is generally assumed that hydrogen is non-reactive at temperatures below 100°C even at high pressures. Recent experiments performed with spent fuel, a potential catalyst, and high H_2 pressures suggest that hydrogen is far more reactive than previously believed (RÖLLIN et al. 2001), thus leading to very low Eh conditions at the spent fuel water interface. The reactivity of hydrogen in the bentonite backfill is virtually unknown and there are, to our knowledge, no experimental data available which would shed light on this matter.

Uranium phases: The radiolytic dissolution of fuel waste leads to oxidation of UO_2 to soluble U(VI) which may move out and interact with the steel corrosion products only if H_2 is non-reactive. According to the model of JOHNSON & SMITH (2000) U transport will extend at the most to the inner part of the bentonite. Sorption of uranyl onto corrosion products may lead to partial blocking of sorption sites and thus inhibit some redox reactions (KING & STROES-GASCOYNE 2000). It is unlikely, however, that equilibria involving uranium phases will play a significant role in controlling of redox conditions in the bentonite porewater because we expect only small amounts of oxdised uranium in the canister and bentonite environment.

3.3 Opalinus Clay host rock

Both Eh-measurements and modelling data indicate that porewaters in Opalinus Clay are reducing. The measured redox potentials are partly conflict with the abundance of unaltered pyrite, which is interpreted as measuring artefact (PEARSON et al. 1999; PEARSON 2002). PEARSON et al. (1999) suggest that the minimum measured Eh-values (-0.1 to -0.3 V) are controlled by the pyrite/sulphate equilibrium. The redox conditions in the host rock will affect those in the backfill material, at least in the outer part, by diffusion of reduced species, such as Fe(II). The HS^- concentration is low in the Opalinus Clay water and below detection limits (~ 10^{-8} M). Based on modelling results PEARSON (2002) suggests that HS^- concentrations are in the range of 10^{-10} - 10^{-11} M.

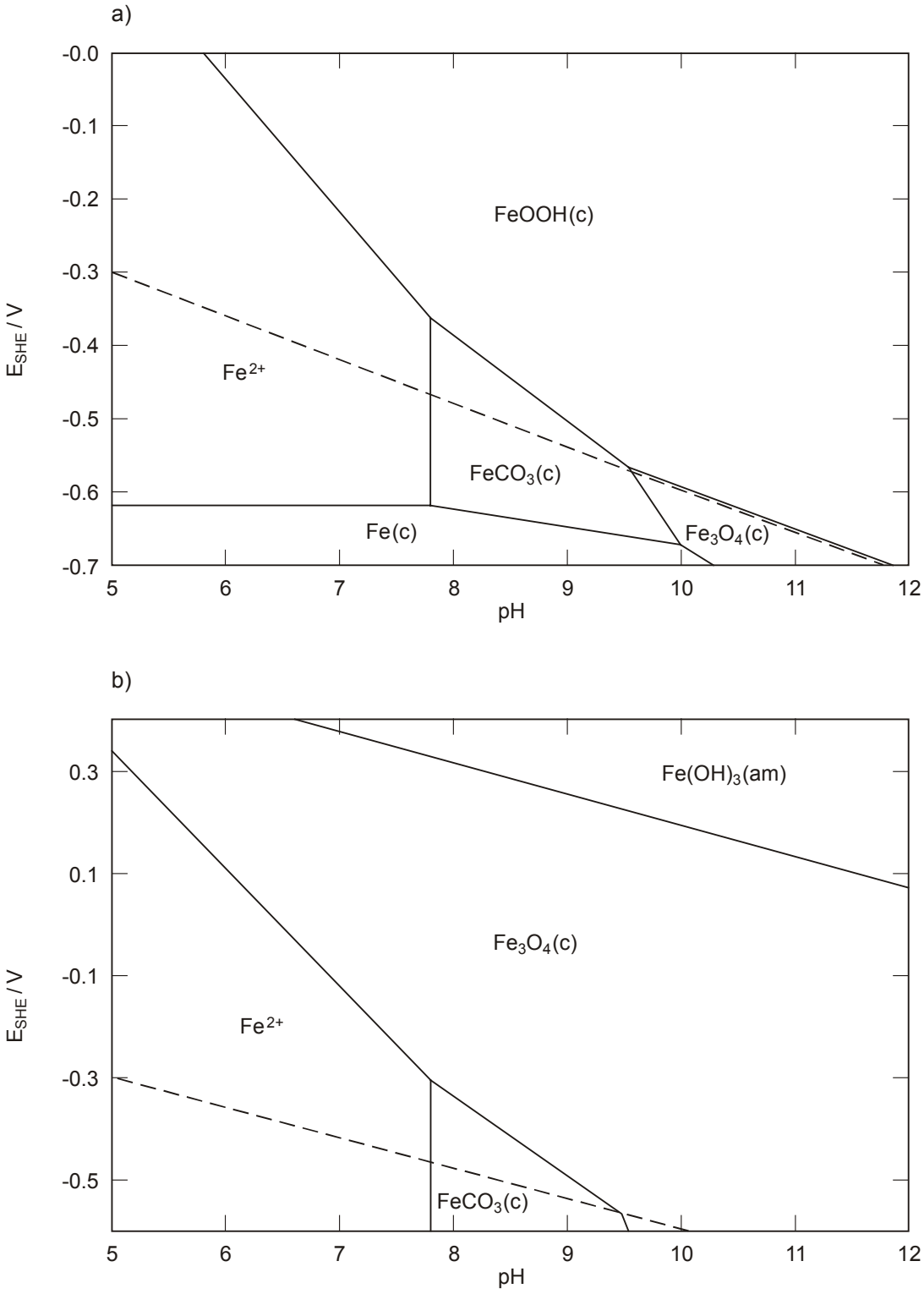

Figure 3.2: Stability field of iron phases in Eh-pH diagram in Fe-CO_2-SO_4-H_2O system.

I = 0.2 mol/L, $[CO_3]_{tot} = 5 \cdot 10^{-4}$ mol/L, [Fe] = $5 \cdot 10^{-6}$ mol/L, $[SO_4] = 10^{-2}$ mol/L, T = 25°C. Sulphate reduction suppressed. Thermodynamic data from HUMMEL et al. (2002). Broken line: H_2O/H_2 eq. (pH_2 = 1 bar) Assumption of formation of goethite, FeOOH(c). b) Assumption of formation of metastable $Fe(OH)_3$(am).

4 Indications from radionuclide reactions

There has been a number of recent experiments carried out to explore the reducing capacity of near field or natural environments with regard to redox-sensitive radionuclides, such as U, Np, Tc and Se. Evidence for reduction of an oxidised species may yield independent evidence for the immobilisation of such elements under near field-like conditions.

Uranium

Sorption and reduction of uranyl have been assessed under neutral to mildly alkaline and anoxic conditions in sulphidic and ferrous systems. (Partial) reduction of U(VI) is rapid in the presence of sulphide surfaces (WERSIN et al. 1994b; MOYES et al. 2000). In reduced iron systems the efficiency of U(VI) reduction seems to depend on the surface reactivity, which is determined by the redox potential at the surface/water interface. U(VI) reduction in magnetite suspensions, if occurring at all, appears to be very slow (GRAMBOW et al. 1996, EL AAMRANI et al. 1999). It should be pointed out, however, that in these experiments commercial magnetite powders were used, which may display surface oxidation and formation to isostructural maghemite (TAYLOR, written communication).

LIGER et al. (1999) showed that extensive reduction occurred at hematite surfaces doped with Fe(II). A number of studies on reactive barriers in groundwaters indicate U(VI) immobilisation in the presence of zero-valent iron (FIEDOR et al. 1998; FARRELL et al. 1999; GU et al. 1998; MORRISON et al. 2001; CANTRELL et al. 1995). CUI & SPAHIU (2002) showed that U(VI) gets rapidly reduced to U(IV) in carbonated solutions in the presence of Fe(0). A key role in this reduction process was assigned to the formation of carbonate-rich green rust at the iron surface which led to a significant increase of reduced U(IV).

Neptunium

So far there are very few experimental data on the redox behaviour of Np(V) in contact with iron mineral surfaces (KING & STROES-GASCOYNE 2000). The few data do not show conclusive evidence for reduction of Np(V). However, a recent study by MOYES et al. (2002) indicates Np(V) reduction on mackinawite, which is a reactive metastable FeS phase.

Technetium

The reduction of Tc(VII) to Tc(IV) in the presence of magnetite and other Fe(II) containing surfaces has been observed in several sorption and diffusion studies which are representative of near-field conditions (e.g. CUI & ERIKSEN 1996; LEE & BONDIETTI 1983).

Selenium

There are very few studies on the reductive sorption of selenate and selenite in the presence of reduced iron surfaces. MYNENI et al. (1997) and JOHNSON & BULLEN (2003) observed reduction of Se(VI) to Se(0) at green rust surfaces. Very recent experimental results of SCHEIDEGGER et al. (2003) indicate reduction of Se(IV) to Se(0) at partially corroded iron surfaces.

In summary, redox-sensitive radionuclides will strongly sorb on magnetite and other Fe(II) surfaces present in the near field. Although the available data are limited to only a few radio-

nuclides relevant to near field conditions, these suggest that corrosion products on the canister surface will promote reduction and immobilisation of redox-sensitive elements such as U(VI), Tc(VIII) and Se(VI/IV). On the other hand, magnetite (not in contact with metallic iron) does not appear to be very reactive compared to green rust phases or other minerals with surface-bound Fe(II).

5 Derivation of redox potentials

5.1 Rationale

The goal of this chapter is to derive reasonable redox potentials for the bentonite porewater at long time scales, to serve as a basis for speciation and solubility calculations of redox-sensitive radionuclides. Given the lack of useful experimental data and the large number of phases and reactions, which could affect redox conditions, this is a difficult task. Nevertheless, the thermodynamic and kinetic considerations presented in the last two chapters help to constrain the system and to limit the number of relevant phases and reactions. These can be summarised as follows:

- Once the initial oxygen is depleted the redox potential in the bentonite porewater will be mainly determined by the very reducing conditions that occur at the interfaces: i.e., the corroded canister and the Opalinus Clay (Fig. 3.1).
- The main thermodynamically stable iron phase formed by steel corrosion is magnetite. Redox potentials at the canister surface are expected to be controlled by magnetite galvanically coupled to Fe^0. Due to limited thermodynamic data, the possible formation of GR is not considered.
- The concentration in the host rock of dissolved Fe^{2+}, which will diffuse into the bentonite, is expected to be rather high. Based on pyrite/siderite equilibrium, the range is 10 -100 μM.
- Recent data indicate that microbially-mediated sulphate reduction is not relevant in compacted bentonite (section 2.2).
- Radiolytic oxidants will affect redox conditions only locally in the vicinity of the waste. The large part of the near field, even under pessimistic assumptions, will remain reducing.
- The high H_2-pressure deriving from anoxic steel corrosion is, due to the limited data on its impact, conservatively assumed not to influence redox conditions.
- The formation of Fe(II)-rich silicates may be of importance at the bentonite - canister and the glass - canister interface, but in view of the lack of experimental and thermodynamic data, the phases are not taken into account for the derivation of redox potentials.

Putting these statements into a thermodynamic framework, we assume that the redox system is controlled by the Fe(III)/Fe(II) couple. This has also been a common assumption in previous performance assessments (CURTI 1993; JOBE et al. 1997). The redox conditions for the Kristallin-I performance assessment (CURTI 1993) were estimated from magnetite/ferric oxide equilibria, which gave rise to rather high oxidation potentials in the case of poorly crystalline ferric oxide. Here we argue against the persistence of a poorly crystalline ferric oxide because:

1. Equilibrium of magnetite with a poorly crystalline ferric hydoxide would lead to an unrealistically low Fe^{2+} activity under the expected geochemical conditions of the pore-water.

2. Ferric oxides are present only in traces in the bentonite material.

3. Experimental data indicate that ferric (hydr)oxides will transform to magnetite in the presence of Fe^{2+} under anoxic conditions (ISHIKAWA et al. 1998).

4. Redox-sensitive metals such as U and Tc would occur in the oxidised form at such high potentials. This is not corroborated by experimental data which suggest the reduction of these elements at repository-like conditions. For example, the redox equilibria for U(VI)/U(IV) and of Tc(VII)/Tc(IV) occur both at oxidation potentials of about 0 mV (SHE) at a pH of 7 (LANGMUIR 1997; our calculations), which is clearly below the stability field of poorly crystalline ferric hydroxide.

From this reasoning we deduce that the redox potential in the vicinity of the canister will be probably controlled by equilibrium of magnetite and Fe(II), the latter originating mainly from diffusion from the host rock. We do not include the lowering of Eh due to galvanic coupling with the steel surface, since farther away from the canister surface this effect may not be relevant and also because radionuclides sorbed to the corroded surfaces may block active sites and thus limit the reducing capacity of the canister environment. The redox potential close to the bentonite-host rock boundary will be determined by that of the Opalinus Clay porewater.

5.2 Thermodynamic modelling

5.2.1 Bases for modelling

Based on the above discussion we assume magnetite/Fe(II) equilibrium to control redox potentials in the near field during the anoxic stage. Dissolved Fe(II) concentrations are assumed to be similar to those of the surrounding clay host rock, as derived from pyrite/siderite equilibrium (PEARSON 2002). From these constraints redox potentials are derived in the bentonite porewater. Additional Fe(III)/Fe(II) equilibria are tested in order to explore their effects on Fe^{2+} activity and Eh. Thus, we test the effect of magnetite/siderite, magnetite/pyrite, goethite[1]/pyrite and siderite/goethite equilibria. Since sulphate reduction is expected to be inhibited, we assume that sulphate and sulphide equilibria are decoupled when assessing chemical reactions involving pyrite. The assumed porewater concentration of HS^- is 10^{-10} M which is the upper range expected in host rock.

Based on the reasoning above the persistence of poorly crystalline ferric oxide is considered to be highly unlikely and thus is not included in the calculations.

Important parameters which influence Eh are pH, ionic strength and ligand concentrations (particularly CO_3^{2-}). These were taken from the modelling study of bentonite porewater chemistry (CURTI & WERSIN 2002). The study defined a "reference water" reflecting the chemically most likely composition, and two alternative waters reflecting bounding cases for pCO_2 and pH. A simplified composition of these waters is given in Table 5.1. An important outcome of that study is that over time scales of interest for performance assessment, the

[1] Goethite is assumed to be the stable Fe(III) oxide phase. Hematite, which might be formed near the canister as a result of high temperatures, is not considered for reasons of simplicity. Including this phase would not affect the general results.

porewater chemistry of the host rock and the bentonite will be similar because of their geochemical and mineralogical similarities.

Thermodynamic redox calculations have been performed with the PHREEQC-2 code (PARKHURST & APPELO 1999) using the NAGRA/PSI Chemical Thermodynamic Data Base 01/01 (HUMMEL et al. 2002) at 25°C. The thermodynamic data for the iron minerals used for the calculations are presented in Table 5.2.

Table 5.1: Porewater composition in mol/L for the bentonite backfill as derived by CURTI and WERSIN (2002).

"Reference water" represents the most likely composition based on chemical understanding, "low pH" and "high pH" represent bounding cases. The apparent positive charge of these waters arises from the modelling approach which does not separate between water that is neutral and bound to the negatively charged clay surface.

	reference water	**low pH**	**high pH**
log pCO_2 [bar]	**-2.2**	-1.5	-3.5
pH	**7.25**	6.90	7.89
Na	$\mathbf{2.74 \times 10^{-1}}$	2.91×10^{-1}	2.49×10^{-1}
Ca	$\mathbf{1.32 \times 10^{-2}}$	1.33×10^{-2}	1.34×10^{-2}
Mg	$\mathbf{7.64 \times 10^{-3}}$	8.91×10^{-3}	6.15×10^{-3}
K	$\mathbf{1.55 \times 10^{-3}}$	1.67×10^{-3}	1.38×10^{-3}
Al	$\mathbf{1.92 \times 10^{-8}}$	1.53×10^{-8}	7.55×10^{-8}
Si	$\mathbf{1.80 \times 10^{-4}}$	1.80×10^{-4}	1.84×10^{-4}
SO_4	$\mathbf{6.16 \times 10^{-2}}$	6.39×10^{-2}	5.59×10^{-2}
CO_3	$\mathbf{2.83 \times 10^{-3}}$	6.99×10^{-3}	5.86×10^{-4}
Cl	$\mathbf{1.66 \times 10^{-1}}$	2.06×10^{-1}	8.61×10^{-2}

Table 5.2: Iron equilibria and logK constants (taken from HUMMEL et al. 2002) used for thermodynamic calculations

Phase	**Reaction**		**$\log K^0$**
Fe^{2+}	Fe^{2+}	$\Leftrightarrow Fe^{3+} + e^-$	-13.02
magnetite	$Fe_3O_4 + 8H^+ + 2e^-$	$\Leftrightarrow 3Fe^{2+} + 4H_2O$	36.06
goethite	$FeOOH + 3H^+$	$\Leftrightarrow Fe^{3+} + 2H_2O$	-1.0[1)]
$Fe(OH)_3$(am)	$Fe(OH)_3 + 3H^+$	$\Leftrightarrow Fe^{3+} + 3H_2O$	3.0
pyrite	$FeS_2 + 2H^+ + 2e^-$	$\Leftrightarrow Fe^{2+} + 2HS^-$	-18.5
siderite	$FeCO_3$	$\Leftrightarrow Fe^{2+} + CO_3^{2-}$	-10.89

[1)] This constant is taken from the work of NORDSTROM et al. (1990). See also footnote no. 4.

5.2.2 Results

The results are presented for a "base case" and two types of variations in Table 5.3. The base case assumes magnetite in equilibrium with a Fe(II) concentration corresponding to that in the clay host rock (4E-5 M) at "reference water" conditions (pH = 7.25). This results in a redox potential of E_{SHE} = -193 mV. The water is slightly undersaturated with respect to siderite.

In variation 1 the effect of pH is evaluated by considering the two limiting porewater compositions shown in Table 5.1. The results indicate that the Eh varies by about 150 mV between the bounding pH values, showing the expected linear inverse relationship with pH. The saturation index (SI[2]) for siderite is close to 0 for the low pH water and -0.8 for the high pH water. The fact that all three bentonite porewaters are not far from equilibrium with regard to siderite is not surprising because of the inherent assumption of Fe(II) being controlled by siderite equilibrium in the host rock which is expected to display similar porewater chemistry to the bentonite backfill.

In variation 2 different Fe(III)/Fe(II) redox buffers, represented by couples of solids in simultaneous equilibria, are considered under the assumption of reference pH/pCO_2 conditions and an initial Fe(II) concentration as in the host rock (4E-5 M). The assumption of magnetite/siderite equilibrium results in a slightly lower Eh than for the base case because of the slightly higher resulting Fe^{2+} activity. The assumption of pyrite/magnetite equilibrium leads to a similar Eh value as for the base case. The assumption of FeOOH in equilibrium with siderite or pyrite results in a significantly lower Eh value[3]. As illustrated in Table 5.3 all other test cases indicate oversaturation with regard to crystalline goethite[4].

[2] SI = log(IAP/K) where IAP is the ion activity product and K the solubility constant.

[3] Note that under the reference water conditions (pH = 7.2) magnetite and goethite do not coexist (cf. Figure 2b) except at unrealistically high Fe^{2+} activities.

[4] The applied stability constant for goethite (also given in NORDSTROM et al., 1990) is probably too low (TAYLOR, written communication). Since this does not put in doubt the conclusions drawn in this report, we did not re-assess the thermodyanmic data of goethite.

Table 5.3: Derived redox potentials in near field of SF/HLW. Various Fe(III)/Fe(II) equilibria assumed (SI = saturation index).

Redox couples	**Geochemical constraints**	**E_{SHE} (mV)**	**Comments**
Base case	*reference water* *pH = 7.25, $pCO_2 = 10^{-2.2}$ bar*		
Fe_3O_4/Fe^{2+}	Fe(II) = 4E-5 M, constrained by Fe(II) in host rock	-193	SI_{FeCO_3} = -0.5, $SI_{goethite}$ = +1.5
Variation 1	*pH variation*		
Fe_3O_4/Fe^{2+}	"low pH" water (pH = 6.9), $pCO_2 = 10^{-1.5}$ bar, Fe(II) = 7E-5 M, constrained by Fe(II) in host rock	-127	SI_{FeCO_3} = +0.1, $SI_{goethite}$ = +1.6
Fe_3O_4/Fe^{2+}	"high pH" water (pH = 7.8), $pCO_2 = 10^{-3.5}$ bar, Fe(II) = 8E-6 M, constrained by Fe(II) in host rock	-282	SI_{FeCO_3} = -0.8, $SI_{goethite}$ = +1.0
Variation 2	*different Fe(III)/Fe(II) equilibria* *pH = 7.25, $pCO_2 = 10^{-2.2}$ bar,* Fe(II) = 4E-5 M		
$Fe_3O_4/FeCO_3$		-202	$SI_{goethite}$ = +1.3
Fe_3O_4/FeS_2	$HS_{tot} = 10^{-10}$ M	-192	SI_{FeCO_3} = -0.1, $SI_{goethite}$ = +1.5
$FeOOH/FeS_2$	$HS_{tot} = 10^{-10}$ M	-271	SI_{FeCO_3} = -0.1, $SI_{Fe_3O_4}$ = -2.7
$FeOOH/FeCO_3$		-277	$SI_{Fe_3O_4}$ = -2.6

5.2.3 Discussion

The thermodynamic calculations performed under the general assumption of redox conditions being controlled by the Fe(III)/Fe(II) couple indicate relatively low Eh values in the range of about -100 to -300 mV. The Eh variations arising from the uncertainty of the nature of the Fe(II)-controlling mineral phases are not very significant. Larger variations arise from uncertainties related to the pH conditions in the bentonite porewater. It should be pointed out that the applied thermodynamic database (Nagra/PSI TDB) predicts magnetite (not contacting the canister) to be thermodynamically less stable in the bentonite porewater relative to siderite/goethite, which would lead to somewhat lower redox potentials.

Green rust formation was not considered due to poor thermodynamic data. Literature data (GÉNIN et al. 1998) suggest that GR may be a stable corrosion product of Fe(0) at circumneutral pH and at high Fe^{2+} activities. Furthermore, other possible Fe(II)-bearing phases which we did not consider because of lack of thermodynamic data are Fe(II)-rich silicate phases. Finally, H_2 gas, which will build up high pressures from the corrosion process, was implicitly assumed to be non-reactive. If H_2 was to play a role in redox reactions, considerably lower redox potentials would be expected.

In summary, we infer that, in spite of a number of uncertainties, redox conditions will remain reducing and are not expected to exceed values of -100 mV. The lower limit of the uncertainty range is, however, difficult to assess, mainly because of the uncertainty related to the behaviour of H_2.

5.3 Kinetics

Redox processes in geochemical systems are often controlled by kinetic factors rather than by thermodynamics. The extent and rate of a reaction are strongly system dependent. This also applies to the redox behaviour of trace elements. Because of lack of data there is a large uncertainty in the redox kinetics of important radionuclides which, from a performance assessment perspective, introduces a further conceptual model uncertainty. Recent experimental data (cf. chapter 5), in particular those on the uranium-iron system, are promising in the sense that they suggest redox behaviour under repository-like conditions consistent with thermodynamic expectations. However, more experimental data are clearly necessary to reduce uncertainties related to the redox kinetics of uranium, neptunium, plutonium, technetium or selenium under repository-like conditions.

6 Conclusions for the SF/HLW case

After a relatively short initial oxic phase the conditions in the bentonite backfill will become and remain reducing. The redox potential will be largely influenced by the corrosion of steel, which will produce large amounts of magnetite, on the internal side of the bentonite barrier, and by the reducing conditions of the surrounding Opalinus Clay, containing siderite and pyrite, on the external side. Although radiolytically enhanced dissolution of the fuel may occur, it is not expected to have a significant impact on redox conditions in the bentonite because of the reactive Fe(II) phases produced by steel corrosion.

The derived Eh range of -100 mV to -300 mV for the anoxic stage mainly reflects the relatively large uncertainties with regard to the pH conditions in the porewater. The uncertainty with regard to Fe(II)-controlling phases does not strongly affect the derived redox potentials and lies within this uncertainty range. The obtained redox conditions are consistent with recent experimental data on the reduction behaviour of U(VI), Tc(VII) and Se(VI/IV).

The possible effect of high hydrogen pressures on redox potentials was not included in our considerations because data on its impact on redox processes occurring in the bentonite is limited. This also holds for iron-rich silicate phases which may play a role at the canister - bentonite boundary, although significant effects on the redox potentials are not expected. Further experimental data on these systems would be useful for future performance assessments.

PART B - INTERMEDIATE-LEVEL WASTE (ILW)

7 General concept of redox evolution

7.1 Waste inventory and redox-sensitive compounds

The layout for the ILW repository, which is described in detail by SCHWYN et al. (2003), is illustrated in Figure 7.1. Low and intermediate-level reprocessing waste is contained in various forms of waste packages. These are put into "Endlager-containers" and filled with mortar. Subsequently, they are stored in three different emplacement tunnels and backfilled with cement. The major part of the waste (ILW-1) will be stored in two parallel tunnels, whereas a small part, containing high amounts of nitrate (ILW-2) will be emplaced separately (SCHWYN et al. 2003). The cement repository is surrounded by the Opalinus Clay host rock. The waste inventory is described in detail by McGINNES (2002).

Both waste types contain predominantly Portland cement and quartz (McGINNES 2002). In addition, relatively high amounts of cement blenders (pulverised fly ash, blast furnace slag) will be present in the BNFL-waste (McGINNES 2002). Steel materials, which make up about 2 - 5 wt% of the total, include waste packages (steel drums, tins, canisters), the reinforced Endlager-containers and the construction materials (anchors, rails, bolts). Small quantities of Al and Zn metals are also present. There is a fairly large amount of organic material in the waste. This is especially true for ILW-2 which contains high levels of bitumen. This waste (COG 4A) is also enriched in nitrate (1%), but, in addition, includes significant amounts of sulphide and cyanide. The quantities and types of wastes discussed in this report correspond to the "cemented waste" option (NAGRA 2002a). Temperatures within an ILW tunnel are not expected to exceed 50°C (JOHNSON et al. 2002).

Both waste types contain high proportions of reduced iron, as is illustrated in Table 7.1. The waste package materials (canisters etc.) are made of stainless steel which show very low corrosion rates under alkaline conditions. In contrast, the other steel materials, such as the reinforcement, anchors, rails and bolts will corrode more readily under cementitious conditions. There are other elemental metals in the waste, such as zinc and aluminium (McGINNES 2002), which will be far more reactive than iron. The cement and blenders have a considerable proportion of iron (Table 7.1). Most of this iron is oxidised and thus the reducing capacity (cf. SCOTT & MORGAN 1990) of these cementitious materials is low. On the other hand, there is a fairly large amount of organic material in the waste. This is especially true for ILW-2 which contains high levels of bitumen. In addition, this waste (COG 4A) is enriched in nitrate, but also contains significant amounts of sulphide and cyanide. The initial O_2 concentration, calculated from an average porosity of ~0.3, is about 160 mol per m of tunnel length for ILW-1 and about 60 mol per m for ILW-2.

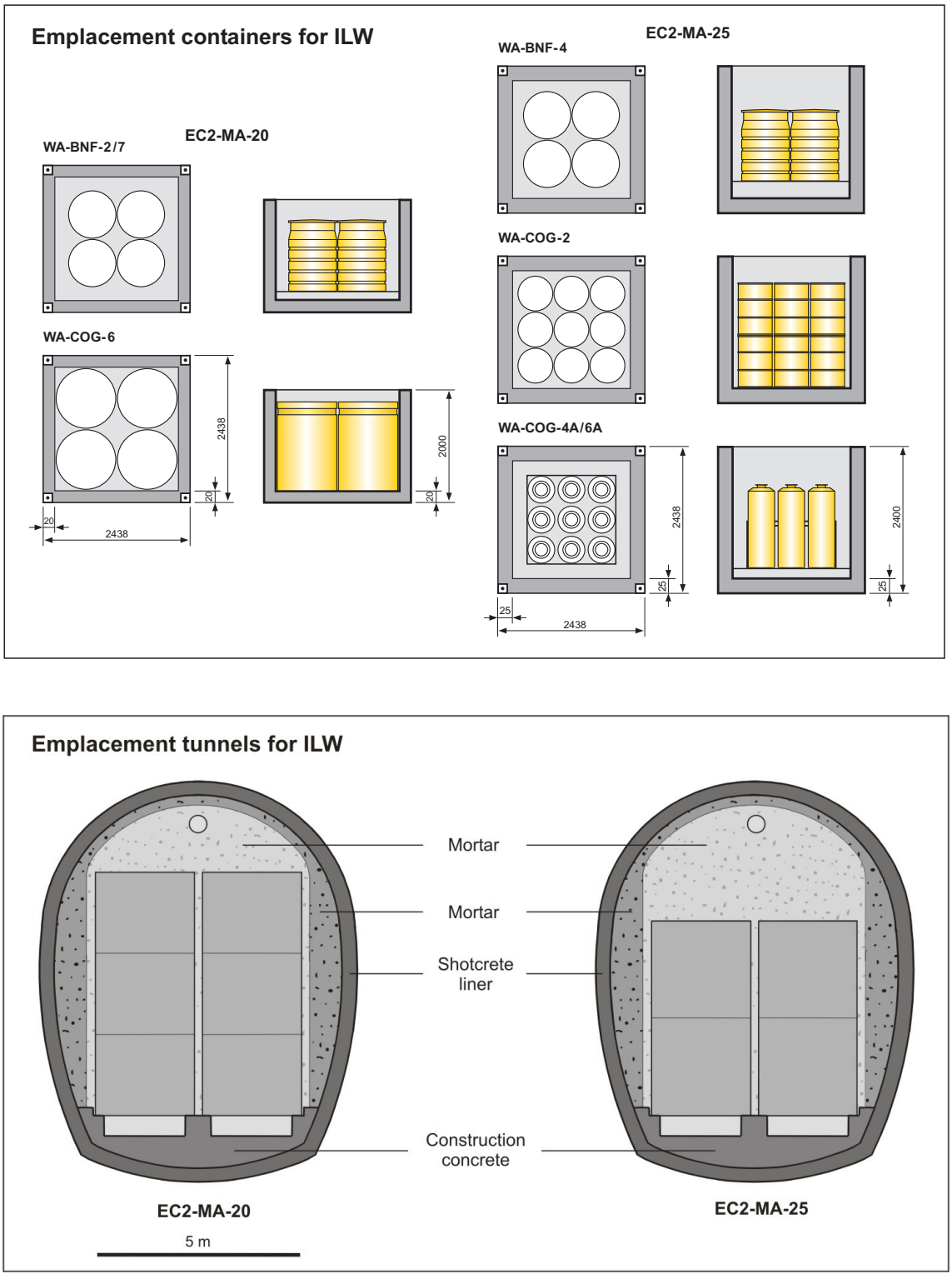

Figure 7.1: Disposal schema for ILW.

Various metallic waste packages are emplaced in concrete containers filled with cement (upper figure).These containers are emplaced in tunnels and backfilled with mortar (lower figure).

The redox capacity (amount of reducible and oxidisable species) of ILW-1 and ILW-2 differs considerably (Table 7.1). ILW-1 contains high-levels of reduced iron and organic carbon. The reducing capacity is decreased by the oxidised Fe present in the cement. The nature of iron phases in cement is poorly known. Some of the iron will be included in iron oxide phases while some may be present as Fe(II) and Fe(III) in Ca-aluminate/ferrite solid solutions. According to our understanding, the cement matrix will be rather inert and not significantly affect redox conditions.

ILW-2 has a high nitrate content (1%) which leads to a high oxidising capacity. On the other hand, this waste also contains considerable amounts of reduced species, i.e. organic carbon and sulphide (Table 7.1).

Table 7.1: Redox inventory of ILW-1 and ILW-2 (calculated from SCHWYN et al. 2003)

Concentrations given in moles of reductant/oxidant per meter of tunnel.

	ILW-1 mol/m	**ILW-2 mol/m**	**dominant oxidation state**	**Comments**
Iron				
waste (canisters)	6×10^4	2×10^3	Fe(0)	high quality steel
construction mat. (rebar, anchors)	3×10^4	6×10^3	Fe(0)	low quality steel
cement	4×10^3	1×10^3	Fe(III)	1% Fe (ATKINS et al. 1993)
cement blender[1]	2×10^3	0	Fe(III)	6% Fe (ATKINS et al. 1993)
Other				
Initial molecular oxygen	1.6×10^2	6.3×10^1	O(0)	calc. from porosity = 0.3
bitumen	0	3×10^4	C(0)	assumed to be $\{CH_2O\}$ units
plastics	6×10^2	4	C(0)	assumed to be $\{CH_2O\}$ units
sodium nitrate ($NaNO_3$)	7	2×10^3	N(V)	
cobalt sulphide (CoS)	0	4×10^2	S(-II)	

[1] pulverised fly ash (PFA)

7.2 Oxic stage

Initially, the redox conditions will be oxidising because of residual oxygen which is entrapped in the pores of the cementitious repository and the excavation-damage zone (EDZ). Oxygen will react predominantly with steel in the near field and reduced mineral phases (e.g., pyrite) in the EDZ. In the case that significant microbial activity occurs, degradation of organic compounds will enhance oxygen consumption.

O_2-consumption rates strongly depend on the degree of saturation in the near field, which is influenced by the hydraulic conductivity of the surrounding rock. The time scales for O_2 depletion can be roughly estimated by assuming three limiting cases: unsaturated, with or without sufficient humidity to cause corrosion, and fully saturated.

1) Unsaturated conditions, with sufficient humidity to cause corrosion

The emplacement of large quantities of cement-based mortar around the canisters during final closure of the repository will result in high relative humidity conditions within the ILW disposal tunnels even if inflow of groundwater is extremely slow. Under high pH conditions, the corrosion rate of mild steel used in the reinforcement, rails and other applications is about 0.1 µm/a and, because of passivation, the rate is the same for both aerated and anoxic conditions (KREIS 1991). It is expected that corrosion will occur as long as the relative humidity exceeds 30 to 40% (MANSFELD & KENKEL 1976).

The rate at which oxygen will be consumed can be calculated according to the procedure given in Appendix A. Since diffusion is fast in unsaturated cement the rate of consumption can be directly related to the corrosion rate of steel. The obtained time of oxygen consumption is about 700 years.

2) Unsaturated conditions, with insufficient humidity to cause corrosion

It is possible that, in the period immediately after mortar emplacement, the activity of water (and therefore the relative humidity) is reduced by the strong affinity of hydrated cement phases for water. Under such conditions, corrosion of steel would probably be negligible, thus oxygen would be available for other reactions. As a result it may diffuse to regions of higher humidity where redox reactions may take place, e.g. pyrite oxidation in the EDZ. The oxygen consumption can be estimated for this case by an analogue treatment as used for the SF/HLW case (see Appendix A). For ILW-1, this calculation leads to a range of 20 - 900 years for oxygen depletion, where the lower range reflects geochemically more realistic conditions (Appendix A). Because of the smaller tunnel cross-section for ILW-2 the corresponding calculation leads to more rapid oxygen depletion (Appendix A).

It is difficult to see how oxidative corrosion of waste and transport of radionuclides (except ^{3}H and possibly ^{14}C) could occur under such conditions, as condensed water would be unavailable in the waste containers.

3) Fully saturated conditions

This is a condition that is not expected for many decades or even longer, given the low permeability of the Opalinus Clay. If fully saturated conditions arose, however, the corrosion rates would be the same as in Case 1.

The results indicate that the flux of O_2 strongly depends on the degree of saturation of the near field. The O_2 consumption is estimated to occur within a couple of hundreds of years. Faster consumption rates are expected in the case of microbial activity. However, since the role of microbial processes is uncertain at present, we have not included them in our time scale estimations. The main pathway for the O_2 flux is most likely diffusion and reaction in the host rock. Under these conditions of a strongly unsaturated near field very low corrosion of the waste is expected.

7.3 Anoxic stage

After oxygen depletion the ILW repository will remain anoxic. Redox conditions will be affected by a number of reactions that occur between the dissolved and solid redox-active materials in the alkaline environment. Corrosion of steel and, to a minor extent, of other reduced

metals will generate high hydrogen pressures. The corrosion of steel will produce magnetite (e.g., KREIS 1991; NAISH et al. 1990; MATSUDA et al. 1995). Dissolved redox-sensitive species (e.g. Fe(II), sulphide) will diffuse from the surrounding reduced host rock and also contribute to the reducing environment in the cement porewater.

Dissolution of residues of uranium-rich fuel which mainly derives from the compacted hulls and ends will lead to radiolytic oxidants and thus potentially to an increase in redox potentials (Eh). Radiolysis will be strongly influenced by concomitant steel corrosion (cf. section 3.2). Moreover, the build-up of high hydrogen pressures may result in significant suppression of oxidative radiolysis effects (SPAHIU et al. 2000).

The high nitrate content in the separate ILW-2 has a high oxidising capacity. On the other hand, this waste also contains large amounts of reduced species, such as sulphide and organic carbon. The redox conditions of ILW-2 are discussed in section 8.3.

Organic materials (e.g., cement additives, bitumen, cellulose) constitute a large source of oxidisable material and a nutrient source for microbial activity. Thus, in principle, microbially-induced degradation of organics may lead to very reducing conditions (section 8.3).

8 Discussion of different redox processes

8.1 Anoxic corrosion of steel

Corrosion rates of low quality steel (i.e, from construction materials) have been reported to be less than 0.1 μm/a (GRAUER 1988; FUJISAWA et al. 1997; KREIS 1991). Rates are affected somewhat by the nature and concentrations of dissolved anions. Elevated Cl-concentrations, such as those that will be present in the ILW porewater (SCHWYN et al. 2003), may increase corrosion rates slightly (NAISH et al. 1990). Assuming a corrosion rate of 0.1 μm/a the oxidation rate per metre of tunnel length is:

10^{-7} m/a x 23.5 m^2 x $7.86 \cdot 10^6$ g/m^3 x 1/55.847 mol/g = 0.33 mol/a

where 23.5 m^2 corresponds to the steel surface area per m^2 (NOLD 2000). At this rate the total low quality steel inventory (30 kmol/m) would corrode after about 90'000 years.

The corrosion process leads to magnetite and hydrogen formation:

$3Fe + 4H_2O \rightarrow Fe_3O_4 + 4H_2$

Due to galvanic coupling of magnetite and elemental Fe the redox conditions close to steel surfaces will be very reducing (KING & STROES-GASCOYNE 2000).

8.2 Dissolution of fuel waste

Relatively high amounts of fuel remnants (with an alpha-residue of about $3 \cdot 10^{11}$ Bq/container) occur in the compacted hulls and ends. The resultant radiolytically produced species have a significant oxidising capacity. The following simple mass balance calculation indicates that there is sufficient reduced iron in the container to consume all oxidant eventually produced by alpha radiolysis of fuel remnants:

Using a very conservative G-value of 1 for H_2O_2 production, and assuming that 50% of the total energy from each disintegration is absorbed by water, the rate of oxidant production (P) is:

$3 \cdot 10^{11}$ Bq x 5 MeV/Bq x 0.5 x 10^6 ev/MeV x 1 H_2O_2 molecule/100 eV = 7.5×10^{15} molecules/s

Hence the production rate at t = 1 a is 0.39 mol/a

The time dependency of alpha decay on the hulls can be assumed to very similar to the one for spent fuel. Based on the above production rate the time dependence of oxidant production (P) in spent fuel, illustrated in JOHNSON & SMITH (2000) can be approximated by:

$P = 0.39\ t^{-0.49}$

This leads to an integrated oxidant production, P_T, from e.g. 1 to 100'000 years of:

$P_T = \int P dt = 0.76[(10^5)^{0.51} - 1^{0.51}] = 269$ mol.

Assuming the steel inventory in a container is ~100 kg (1820 mol), mass balance considerations show that there is sufficient reduced iron to consume all oxidants produced by radiolysis, even assuming a conservative G-value of 1.

In the case that radiolysis outlasts steel corrosion it might affect redox potentials. The only oxidant that is expected to be relevant is uranyl (HEATH & TWEED 1999), since other produced species, such as O_2 and H_2O_2 are rapidly reduced by the fuel materials or the iron corrosion products. The small amounts of UO_2^{2+} generated by radiolysis after completion of steel corrosion will presumably be reduced by the large amounts of reduced iron, still present in the corrosion products, i.e. mainly magnetite (GRAUER 1988).

8.3 Microbially-induced processes

Cement is a hostile environment to microbial life because of its alkaline conditions and, in case of concrete also because of its pore structure. Microbial studies at the Maqarin site that serves as natural analogue for altered cement indicate low bacterial counts and low biodiversity (PEDERSEN 1997). According to WENK (1993) microbial activities cannot be excluded under cementitious repository conditions because alkaline resistant fermenting bacteria may create niches for less resistant ones. In summary, microbial activity cannot be ruled out in the ILW repository but is expected to be low.

Organic matter degradation

The waste contains large amounts of organic compounds, which constitute a high source of energy or a high reducing capacity. The degradation of organic matter, however, requires microbial activity. From a chemical point of view oxidation of C necessitates electron acceptors which, after O_2 depletion, will include nitrate, Mn(II), Fe(II), and possibly SO_4 and C(IV) (STUMM & MORGAN 1996). The redox reactions can be schematically represented as:

$\{CH_2O\} + Ox \rightarrow CO_2 + H_2O + Red$

where $\{CH_2O\}$ represents the average organic matter and "Ox" represent the oxidised and "Red" the reduced species, respectively.

For the majority of the waste disposed in ILW-1, the long-term supply of nitrate, Mn(II) and Fe(II) is limited by diffusion from the Opalinus Clay. The separately disposed ILW-2 waste contains large amounts of nitrate and thus a high oxidising capacity which may lead to oxidising conditions, provided that nitrate reducing bacteria are active, as discussed below.

The degradation rate of organic materials for both waste types is expected to be low and thus will not significantly affect redox potentials (GRAUER 1988; NEALL 1994). According to NEALL (1994), degradation of organic matter may affect redox conditions after longer time periods, after the steel corrosion process has been completed.

The assumed low degradation rate of organic materials is in apparent contradiction with the ones used for calculating gas production rates (NAGRA 2002a). This, however, is explained by the different focus of that work where high degradation rates were assumed for obtaining pessimistic estimates of gas production rates. If similar degradation rates were assumed for estimation of redox conditions then rapid O_2 consumption would occur and very low Eh values would result.

Nitrate reduction in ILW-2

As mentioned above, the high nitrate content (2 kmol/m tunnel) constitutes a high oxidising capacity. On the other hand, this compares to about 8 kmol of elemental Fe, about 0.4 kmol of sulphide and about 30 kmol of organic carbon from the bitumen filling material. Thus, in principle, there is a large excess of reduced species compared to nitrate. However, it will be the kinetics of the different redox reactions that will determine whether nitrate reduction will significantly affect redox conditions. Moreover, the high concentration gradient will induce nitrate diffusion to the host rock. In case of low microbial activity the rate of nitrate decrease reduction may be diffusion limited. It is noteworthy, however, that experiments (KILEMOES et al. 2000) suggest that chemically induced denitrification leading to slightly enhanced iron corrosion may occur. If such a process was important nitrate depletion would occur within short time scales.

8.4 Diffusion of reduced species from the host rock

The porewaters of Opalinus Clay are reducing. As pointed out in section 3.3, PEARSON (2002) suggests that redox potentials are controlled by the pyrite/sulphate equilibrium based on geochemical data and modelling results. Diffusion of Fe(II) and HS^- to the cement repository will occur and thus contribute to the reducing environment in the repository. The dissolved concentrations of these species will, however, be very low in the alkaline repository.

9 Estimation of redox potentials

9.1 Bases for model calculations

As has been discussed in the previous section, the redox conditions in the chemically heterogeneous alkaline environment will be affected by thermodynamic as well as kinetic factors. In spite of considerable uncertainties, redox potentials can be constrained on the basis of the considerations summarised below. Because the small ILW-2 subrepository contains different redox-active compounds relative to the main ILW-1 subrepository, it will be treated separately.

9.1.1 ILW-1

From the preceding discussions the following statements are deduced:

- The reducing capacity of the repository components is very large because of the high amounts of steel and organic compounds. The only process after depletion of residual O_2 that may potentially lead to higher redox potentials is radiolysis arising from U-bearing waste in the compacted hulls and ends.
- Steel corrosion is likely to be the principal process governing redox conditions. This is in accordance with the outcomes of previous assessments of intermediate-level cementitious repositories (HEATH & TWEED 1999; KARLSSON et al. 1999). Steel corrosion will lead to the formation of magnetite, which is the thermodynamically stable iron phase under these conditions (cf. section 9.1.4).
- As indicated from mass balance calculations radiolysis is not expected to notably affect redox conditions as long as steel corrosion persists, even under pessimistic assumptions.
- Microbial activity and concomitant degradation rates of organics are expected to be low compared to steel corrosion. It must be pointed out that considerable uncertainties exist with regard to the role of microbes in such an environment. Degradation of organic matter might be important once steel corrosion is completed. In this case low redox potentials are expected (iron-reducing, sulphate-reducing or even methanogenic).
- The build-up of high H_2-pressures deriving from steel corrosion is assumed, due to the limited data on its impact, not to influence redox potentials.
- After long time periods, when steel corrosion is completed, it has been suggested (NEALL 1994) that the radiolytically-produced oxidant UO_2^{2+} may increase redox potentials. This effect, however, in our view, is probably not relevant because oxidant production will be low and UO_2^{2+} may be reduced chemically at corroded surfaces.

From this current picture we deduce, in agreement with previous studies, that redox potentials will be largely influenced by the steel corrosion process which yields magnetite as principal corrosion product. Based on this finding and on previous work (GRAUER 1988; HEATH & TWEED 1999) we estimate Eh values by considering Fe(III)/Fe(II) equilibria as discussed in section 10.1.4.

9.1.2 ILW-2

The fate of nitrate in such a complex environment is uncertain. If there is low microbial activity and low chemical reactivity with regard to reducing agents (e.g., steel, sulphide), then similar redox conditions as for ILW-1 will hold. If nitrate reduction occurs, its effect on redox potentials will depend on the kinetics of the different redox reactions taking place. High oxidation potentials might occur in case nitrate reduction is relatively fast compared to steel corrosion. However, in this case nitrate would be depleted within short time scales. If the rate of nitrate reduction is low, it may outlast steel corrosion and have the potential to affect redox conditions over long time scales. Given this uncertainty we conservatively assume redox potentials to be controlled by the N(V)/N(0) redox couple.

9.1.3 Porewater compositions

The cement porewater chemistry has been assessed by SCHWYN et al. (2003) on the basis of a thermodynamic cement model (BERNER 1990; NEALL 1994). Thus, three stages (so-called "regions") have been derived: region I corresponds to the initial stage characterised by very high

pH values of about 13.5 dominated by alkali hydroxides; region II corresponds to the stage controlled mainly by the portlandite equilibrium, with pH values of about 12.5; region III corresponds to a stage dominated by the dissolution of CSH phases. According to the modelling results, it can be inferred that alkaline conditions, in particular region II, will persist for very long time periods (and those relevant for performance assessment) because of the low exchange rate with the surrounding argillaceous formation water. Table 9.1 gives simplified compositions of the initial phase water and region II water. Because of its long persistence the latter water is referred to as "reference water" for the main ILW-1 repository (SCHWYN et al. 2003). ILW-2 will have similar composition of major compounds except for its high nitrate content (Table 9.1).

Table 9.1: Porewater composition for ILW-1 and ILW-2

Concentrations in mmol/L. (cf. SCHWYN et al. 2003).

	ILW-1		**ILW-2**
	region I initial stage	**region II "reference water"**	**region II "reference water"**
pH	13.44	12.55	12.55
Na	101	169	669
K	303	5.7	5.7
Ca	0.84	20.1	20.1
Mg	$<10^{-4}$	10^{-4}	10^{-4}
Al	0.01	0.005	0.005
CO_3	0.20	0.01	0.01
SO_4	0.75	0.1	0.1
Cl	-	160	160
SiO_2	0.05	0.016	0.016
NO_3			498

9.1.4 Redox control by iron phases

Corrosion studies performed under anaerobic conditions (e.g., BÜCHLER et al. 1998) indicate the formation of a thin passive film with composition of a spinel-type $Fe_{3-x}O_4$ phase. The exact mineralogical and chemical composition of this phase is still poorly known but strongly depends on applied solution conditions. It has been suggested that under strictly anoxic conditions and long time scales magnetite will be formed at the steel surface (e.g., GRAUER 1988). Other potential iron(II)-bearing corrosion products under alkaline conditions are $Fe(OH)_2$ (e.g., WINKLEHAUS et al. 1966) and Fe(III)/Fe(II) green rust type phases. Furthermore, pyrite formation should be considered in the cementitious repository, especially in case that microbial sulphate reduction would occur.

On the other hand, the main iron fraction in the cement matrix is Fe(III) (Table 7.1). The nature of these iron(III)-bearing phases and especially their reactivity with regard to redox reactions is poorly known, but Fe(III) oxides (respectively hydrous ferric oxides) constitute a significant fraction thereof. Fe(III) oxides display a wide range of thermodynamic stability depending on their crystallinity and structure. Degradation experiments performed with cement pastes

(SAROTT et al. 1995) indicate maximum dissolved Fe concentrations of about 10^{-7} mol/L. This value may serve as a constraint for an upper solubility limit of Fe(III) in the cement matrix.

Based on the above considerations redox conditions were evaluated under the assumption of redox control by Fe(III)/Fe(II) mineral equilibria. The different considered mineral phases and their equilibrium constants are listed in Table 9.2. The thermodynamic data were taken from the NAGRA/PSI Chemical Thermodynamic Data Base 01/01 (HUMMEL et al. 2002). For ferrous hydroxide logK was taken from STUMM & MORGAN (1996).

Table 9.2: Solid iron phase equilibria used for thermodynamic calculations.

Mineral phase	**Reaction**	**logK^0**	**Reference**
magnetite	$Fe_3O_4 + 8H^+ + 2e^- \Leftrightarrow 3Fe^{2+} + 4H_2O$	36.06	HUMMEL et al. (2002
goethite	$FeOOH + 3H^+ \Leftrightarrow Fe^{3+} + 2H_2O$	-1.0	HUMMEL et al. (2002)
hematite	$Fe_2O_3 + 6H^+ \Leftrightarrow 2Fe^{3+} + 3H_2O$	1.12	HUMMEL et al. (2002)
$Fe(OH)_3$(am)	$Fe(OH)_3 + 3H^+ \Leftrightarrow Fe^{3+} + 3H_2O$	3.0	HUMMEL et al. (2002)
pyrite	$FeS_2 + 2H^+ + 2e^- \Leftrightarrow Fe^{2+} + 2HS^-$	-18.5	HUMMEL et al. (2002)
troilite	$FeS + H^+ \Leftrightarrow Fe^{2+} + HS^-$	-5.31	HUMMEL et al. (2002)
siderite	$FeCO_3 \Leftrightarrow Fe^{2+} + CO_3^{2-}$	-10.89	HUMMEL et al. (2002)
Fe(II)hydroxide	$Fe(OH)_2 + 2H^+ \Leftrightarrow Fe^{2+} + 2H_2O$	12.9	STUMM & MORGAN (1996)

The stability of Fe species at repository conditions is visualised by an Eh-pH diagram constructed on the basis of iron equilibria and expected porewater concentrations and under the constraint of no sulphate reduction reactions or methane formation. As is illustrated in Fig. 9.1a, magnetite and goethite are the thermodynamically stable iron minerals in the expected Eh-pH field. Due to low carbonate activity in the cementitious repository, siderite is not expected to be stable. This is also the case for ferrous hydroxide (Figure 9.1), which has been suggested by HEATH & TWEED (1998) to control Fe^{2+} in a cementitious repository. However, because of the high uncertainties in available logK-values for ferrous hydroxide, the thermodynamic stability of $Fe(OH)_2$ should be further evaluated. If sulphate reduction reactions are included pyrite becomes stable at neutral and weakly alkaline conditions whereas FeS remains metastable under realistic porewater chemistry conditions (data not shown). Because of these findings $Fe(OH)_2$, $FeCO_3$ and FeS were not further considered for the calculation of redox potentials which are described subsequently.

It should be noted that transformation of Fe(III) is slow and may be governed by kinetic factors. Thus, the persistence of metastable phases over long time scales cannot be discarded, especially under alkaline conditions where the concentrations of redox-active species in solution is very low. In case of persistence of metastable ferrihydrite the stability field of magnetite is markedly increased (Figure 9.1b).

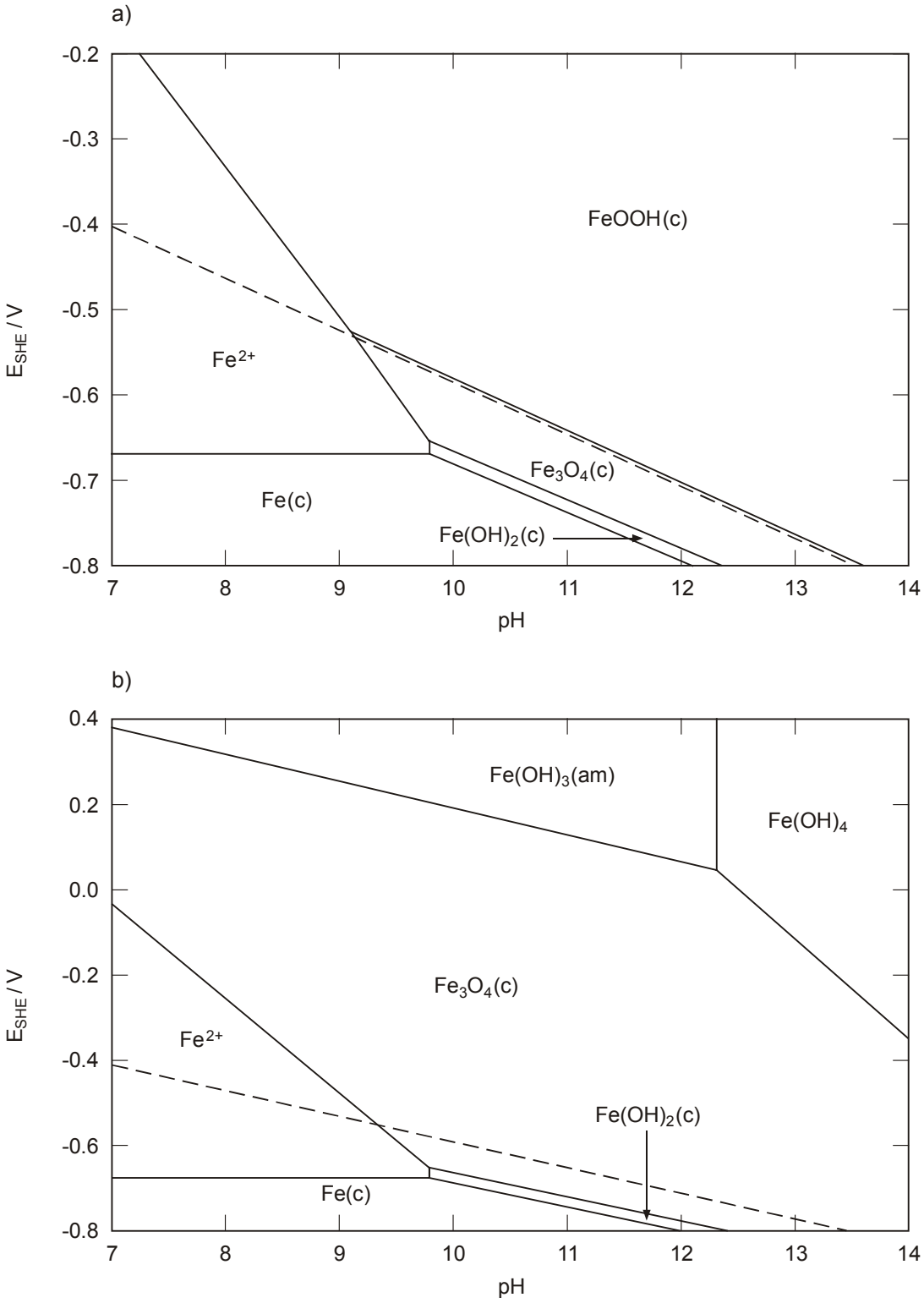

Figure 9.1: pH-Eh diagram for the Fe-CO_2-H_2O system.

Thermodynamic data from Table 9.1 and NAGRA/PSI thermodynamic database, T = 25°C. Dashed line: H_2O/H_2 eq. a) assuming goethite, FeOOH(c) as stable Fe(III) oxide b) assuming $Fe(OH)_3$(am) as stable Fe(III) oxide.

For the derivation of redox potentials different Fe(III)/Fe(II) redox couples were assumed in order to estimate the range of Eh for a cementitious porewater. Thus, a number of test cases were run (Table 9.3). This also included a hypothetical FeOOH phase in cement regulating Fe^{3+} activity in agreement with the above mentioned experimental data of SAROTT et al. (1995), i.e. $Fe(III)_{tot} = 10^{-7}$ M. Furthermore, the effect of sulphate reduction and resulting pyrite formation was tested. The different test cases are presented in Table 9.3. Calculations were primarily done for the "reference" porewater of ILW-1, which corresponds to region II (i.e. pH = 12.55), as presented in the last section.

9.2 Results for ILW-1

The results are illustrated in Table 9.3. The assumption of magnetite in equilibrium with crystalline goethite (the thermodynamically stable phase assemblage, see also Figure 9.1a) results in a very low E_{SHE} value of -742 mV at the imposed pH of 12.55. The assumption that metastable Fe(III) hydroxide phases persist and control Fe^{3+} activities strongly affects redox conditions. Thus, the assumption of $Fe(OH)_3$(am) and magnetite equilibrium results in an Eh value of -32 mV. Assuming however that magnetite is in equilibrium with a FeOOH phase that limits Fe(III) concentrations constrained by Fe(III) = 10^{-7} M (FeOOH(cem)), as suggested by the data of SAROTT et al. (1995), gives rise to an Eh value of -226 mV. Under the assumption that sulphate reduction and concomitant pyrite formation occurs, considerably lower Eh values in the range of -570 to -590 mV result (Table 9.3). The Eh values derived for the initial high pH stage (i.e. pH 13.44) are also presented in Table 9.3 for the magnetite in equilibrium with goethite and with a solution having $Fe_{tot} = 10^{-7}$ M.

Table 9.3: Test runs for different Fe(III)/Fe(II) equilibria for ILW-1.

Fe(III)/Fe(II) equilibria	**E_{SHE}** (mV)	**Fe(III)** (M)	**Fe(II)** (M)	**Comments**
A) pH =12.55 (region II)				
no sulphate reduction				
magnetite-goethite	-742	1.2E-10	1.3E-10	thermodynamically stable assemblage (excluding hematite eq.)
magnetite- $Fe(OH)_3$(am)	-32	1.2E-06	insign.	$SI_{goethite} = +4.0$
magnetite-FeOOH(cem)*	-226	1.0E-07	insign.	$SI_{goethite} = +2.9$
incl. sulphate reduction				
magnetite-pyrite	-588	2.3E-12	8.8E-10	$SI_{goethite} = +0.9$
pyrite-goethite	-591	3.5E-13	1.2E-10	$SI_{magnetite} = -2.6$
pyrite-$Fe(OH)_3$(am)	-576	1.2E-06	1.9E-09	$SI_{magnetite} = +9.2$, $SI_{goethite} = +0.9$
pyrite- FeOOH(cem)*	-580	1.9E-10	1.0E-07	$SI_{magnetite} = +6.0$, $SI_{goethite} = +0.9$
B) pH =13.44 (region I)				
magnetite-goethite	-790	8.4E-10	3.7E-06	
magnetite-FeOOH(cem)*	-432	1.0E-07	3.4E-10	$SI_{goethite} = +2.0$

* hypothetical FeOOH phase regulating Fe(III) conc. at 10^{-7} M

In summary, under the assumption of Fe(III)/Fe(II) equilibrium, the derived Eh conditions are very dependent on the crystallinity of the Fe(III) oxide. In our view, the only indication for constraining the upper limit are experimental data which indicate Fe(III) concentrations < 10^{-7} M. This leads to an upper Eh value of about -230 mV. If sulphate reduction was important significantly lower Eh values would be expected. Lower redox potentials are also obtained for the initial high pH phase.

It is important to note that in the calculated upper Eh range (-200 to -300 mV) the oxidised U(VI) would be the stable redox state. As mentioned in section 9.1.1, this is considered unlikely, but cannot be ruled out completely.

The porewater of the cementitious repository will contain very low dissolved iron concentrations. Thus, redox reactions will occur principally via solid phase transformation reactions. This suggests a rather low reactivity with regard to redox reactions compared to the SF/HLW system.

9.3 Results for ILW-2

As discussed in section 9.1.2 redox conditions in ILW-2 are very difficult to assess mainly because of the high uncertainty related to the kinetics of nitrate reduction reactions. In the case of absence of significant microbial processes similar conditions as postulated for ILW-1 are expected to result. In case of significant nitrate reduction rates (but slow enough to be relevant over long time scales) upper redox potentials can be estimated by assuming N(V)/N(0) equilibrium (with $p_{N2} = 10^{-1}$ bar). From this constraint and taking the porewater composition of ILW-2 as described in Table 9.1, an Eh value of +350 mV is obtained. This value is indicative of the assumed highly oxidising capacity of this waste stream.

10 Conclusions for the ILW case

After relatively rapid depletion of residual oxygen the conditions in the LMA-1 repository will remain reducing. The redox potential will be largely influenced by steel corrosion producing thin magnetite-type films on steel surfaces. The redox conditions in ILW-2 are expected to be rather similar; however, they might be more oxidising if high nitrate concentrations persist over long time periods. In case nitrate would decrease to low levels within short time scales, then long-term redox conditions would not be affected by this species.

The uncertainties with regard to the redox potentials in solution are large, mainly because of the lack of unequivocal experimental information on the phases arising in long-term corrosion of steels and the poorly studied role of iron bearing cement phases. In addition, the importance of bacterially induced organic matter degradation, though considered to be of minor importance, is not adequately understood. If significant degradation occurred, lower redox potentials would be expected. This would also be the case if H_2 produced by the corrosion process were more reactive than commonly assumed.

Further experimental work focussing on the corrosion of steel under alkaline conditions as well as the identification of iron bearing phases in the cement repository is needed to improve the understanding of the relevant redox processes. Also, the behaviour of redox-sensitive elements, such as U, Tc and Np should be experimentally investigated.

Acknowledgements

We would like to thank Peter Taylor for his careful review and helpful comments. The comments of Ian McKinley and Erich Wieland on earlier versions of the manuscript are acknowledged. We thank Anne Claudel for the French translation of the abstract. All stability diagrams were constructed with the program package MEDUSA developed by Ignasi Puigdomenech (www.kemi.kth.se/medusa).

11 References

ABDELMOULA M., REFAIT PH., DRISSI S.H., MIHE J.P. & GÉNIN J.-M. R. (1996): Conversion electron Mössbauer spectroscopy and X-ray diffraction studies of the formation of carbonate-containing green rust one by corrosion of metallic iron in $NaHCO_3$ and ($NaHCO_3$ + NaCl) solutions. Corrosion Science 38, 623-633.

ATKINS M., GLASSER F.P., MORONI L.P. & JACK J.J. (1993): Thermodynamic modelling of blended cements at elevated temperature (50 - 90°C). DOE/HMIP/RR/94.011. Her Majesty's Inspectorate of Pollution, London.

BAEYENS B. & BRADBURY M.H. (1995): A quantitative mechanistic description of Ni, Zn and Ca sorption on Na-Montmorillonite. Part I: Physico-chemical characterisation and titration measurements. Nagra Technical Report NTB 95-04, Nagra, Wettingen, Switzerland.

BERNER U. (1990): A thermodynamic description of the evolution of pore water chemistry and uranium speciation during the degradation of cement. Nagra Technical Report NTB 90-12, Nagra, Wettingen, Switzerland.

BÖRGESSON L. & HERNELIND J. (1999): Coupled thermo-hydro-mechanical calculations of the water saturation phase of a KBS-3 deposition hole. SKB Technical Report TR-99-41, SKB, Stockholm, Sweden.

BROWN P.W. & MASTERS L.W. (1982): Atmospheric Corrosion. W.H. Silor (ed.), New York.

BÜCHLER M., SCHMUKI P. & BÖHNI H. (1998): Iron passivity in borate buffer: formation of a deposited layer and its influence on the semiconductive properties. J. Electrochem. Soc. 145, 609-614.

CANTRELL K.J., KAPLAN D.I. & WIESTMA T.W. (1995): Zero-valent iron for the in situ remediation of selected metals in groundwater. J. Hazard. Mat. 42, 201-212.

COLLIN M. & RASMUSON A. (1988): A comparison of gas diffusivity models for unsaturated porous media. Soil Sci. Soc. Am. J. 52, 1559-1565.

CUI D. & ERIKSEN T.E. (1996): Reduction of Tc(VII) and Np(V) in solution by ferrous iron. A laboratory study of homogeneous and heterogeneous redox processes. SKB, Technical Report TR 96-03, SKB, Stockholm, Sweden.

CUI D. & SPAHIU K. (2002): The reduction of U(VI) on corroded iron under anoxic conditions. Radiochim. Acta 90, 623-628.

CURTI E. (1993): Modelling bentonite pore waters for the Swiss high-level radioactive waste repository. Nagra Technical Report NTB 93-45, Nagra, Wettingen, Switzerland.

CURTI E. & WERSIN P. (2002): Assessment of porewater chemistry in the bentonite backfill for the Swiss SF/HLW repository. Nagra Technical Report NTB 02-09, Nagra, Wettingen, Switzerland.

DRISSI S.H., REFAIT PH., ABDELMOULA M. & GÉNIN J.M.R. (1995): The preparation and thermodynamic properties of Fe(II)-Fe(III) hydroxide-carbonate (green rust 1); Pourbaix diagram of iron in carbonate-containing aqueous media. Corrosion Science 37, 2025-2041.

EL AAMRANI F., CASAS I., DE PABLO J., DURO L., GRIVÉ M. & BRUNO J. (1999): Experimental and modelling study of the interaction between uranium(VI) and magnetite. SKB Technical Report TR-99-21, SKB, Stockholm, Sweden.

FARRELL J., BOSTICK W.D., JARABECK R.J. & FIEDOR J.N. (1999): Uranium removal from ground water using zero valent iron media. Ground Water 37, 618-624.

FIEDOR J.N., BOSTICK W.D., JARABECK R.J. & FARRELL J. (1998): Understanding the mechanism of uranium removal from groundwater by zero-valent iron using X-ray photoelectron spectroscopy. Environ. Sci. Technol. 32, 1466-1473.

FUJISAWA, R., CHO T., SUGAHARA K., TAKIZAWA Y., HORIKAWA Y., SHIOMI T., & HIRONAGA M. (1997): The corrosion behaviour of iron and aluminum under waste disposal conditions, Mat. Res. Soc. Symp. Proc. 465, 675-682.

GÉNIN J.-M. R., BOURRIÉ G., TROLARD F., ABDELMOULA M., JAFRECIZ A., REFAIT P., MAITRE V., HUMBERT B. & HERBILLON A. (1998): Thermodynamic equilibria in aqueous suspensions of synthetic and natural Fe(II)-Fe(III) green rusts: Occurrences of the mineral in hydromorphic soils. Environ. Sci. Technol. 32, 1058-1068.

GLAUS M. (2001): Berücksichtigung mikrobieller Effekte in der Sicherheitsanalyse: Welche Informationen können aus der Literatur gewonnen werden? PSI unpubl. Report, TM-44-01-05, PSI, Villigen, Switzerland.

GRAMBOW B., SMAILOS E., GECKEIS H., MÜLLER R. & HENTSCHEL H. (1996): Sorption and reduction of uranium(VI) on iron corrosion products under reducing saline conditions. Radiochim. Acta 74, 149-154.

GRAUER R. (1988) The corrosion behaviour of carbon steel in Portland cement. Nagra Technical Report NTB 88-02E, Nagra, Wettingen, Switzerland.

GRAUER R. (1990): The chemical behaviour of montmorillonite in a repository backfill: selected aspects. Nagra Technical Report NTB 88-24E, Nagra, Wettingen, Switzerland.

GU B., LIANG L., DIECKEY M.J., YIN X. & DAI S. (1998): Reductive precipitation of uranium(VI) by zero-valent iron. Environ. Sci. Technol. 32, 3366-3373.

GUILLAUME D., PIRONON J. & GHANBAJA J. (2001): Valence determination of iron in clays by electron loss spectroscopy. In 12th International Clay Conference, 22-28 July 2001, Bahia Blanca, Argentina.

HEATH T.G. & TWEED C.J. (1999) A model for redox control in a cementitious repository. Mat. Res. Symp. Proc. 556, 1245-1252.

HELLER-KALLAI L. (1997): Reduction and reoxidation of nontronite: the data reassessed. Clays and Clay Minerals 45, 476-479.

HUMMEL W., BERNER U., CURTI E., PEARSON J.F. & THOENEN T. (2002): Nagra/PSI Thermochemical Data Base 01/01. Nagra Technical Report NTB 02-16, Nagra, Wettingen, Switzerland.

ISHIKAWA T., KONDO Y., YASUKAWA A. & KANDON K. (1998): formation of magnetite in the presence of ferric oxides. Corrosion Science 40, 1239-1251.

JOBE D.L., LEMIRE R.J. & TAYLOR P. (1997): Iron oxide redox chemistry and nuclear fuel disposal, AECL-11667, COG-96-487-1, AECL, Canada.

JOHNSON T.M. & BULLEN T.D. (2003): Selenium isotope fractionation during reduction by Fe(II)-Fe(III) hydroxide-sulfate (green rust). Geochim. Cosmochim. Acta 67, 413-420.

JOHNSON L.H. & SMITH P.A (2000): The interaction of radiolysis products and canister corrosion products and the implications for radionuclide transport in the near field of a repository for spent fuel. Nagra Technical Report NTB 00-04, Nagra, Wettingen, Switzerland.

JOHNSON L.H., NIEMEYER M., KLUBERTANZ G., SIEGEL P. & GRIBI P. (2002): Calculations of the temperature evolution of a repository for spent fuel, vitrified high-level waste and intermediate-level waste in Opalinus Clay. Nagra Technical Report NTB 01-04, Nagra, Wettingen, Switzerland.

KARLSSON F., LINDGREN M., SKAGIUS K., WIBORGH M. & ENGKVIST I. (1999): Evolution of geochemical conditions in SFL 3-5. SKB Report R-99-15, SKB, Stockholm, Sweden.

KILEMOES J., DE BOEVER P. & VERSTRAETE W. (2000): Influence of denitrification on the corrosion of iron and stainless steel powder. Environ. Sci. Technol. 34, 663-671.

KING F., QUINN M.J. & MILLER N.H. (1999): The effect of hydrogen and gamma radiation on the oxidation of UO_2 in 0.1 mol.dm^{-3} NaCl solution. SKB Technical Report TR-99-27, SKB, Stockholm, Sweden.

KING F. & STROES-GASCOYNE S. (2000): An assessment of the long-term corrosion behaviour of C-steel and the impact on the redox conditions inside a nuclear fuel waste disposal container. Ontario Power Generation Report No: 06819-REP-01200-10028-R00, Toronto, Canada.

KOSTKA J.E., WU J., NEALSON K.H. & STUCKI J.W. (1999): The impact of structural Fe(III) reduction by bacteria on the surface chemistry of smectite clay minerals. Geochim. Cosmochim. Acta 63, 3705-3173.

KREIS P. (1991): Hydrogen evolution from corrosion of iron and steel in low/intermediate-level waste repositories. Nagra Technical Report NTB 91-21, Nagra, Wettingen, Switzerland.

KUCERA, V. & MATTSON, E. (1987): Atmospheric Corrosion, in *Corrosion Mechanisms,* F. Mansfeld, ed. , New York.

LANGMUIR D. (1997): Aqueous environmental geochemistry. Prentice Hall, Upper Saddle River, New Jersey.

LEE S.Y. & BONDIETTI E.A. (1983): Technetium behaviour in sulfide and ferrous iron solutions. Mat. Res. Soc. Symp. Proc. 15, 315-322.

LIGER E., CHARLET L. & VAN CAPPELLEN P. (1999): Surface catalysis of uranium(VI) reduction by iron(II). Geochim. Cosmochim. Acta 63, 2939-2955.

MÄDER U.K. & MAZUREK M. (1998): Oxidation phenomena and processes in Opalinus Clay: evidence from excavation-disturbed zones in Hauenstein and Mt. Terri tunnels, and Siblingen open pit clay. Mat. Res. Soc. Symp. Proc. 506, 731-739.

MADSEN F.T. (1998): Clay mineralogical investigations related to nuclear waste disposal. Clay Minerals 33, 109-129.

MANSFELD F. & KENKEL J.V. (1976): Electrochemical monitoring of atmospheric corrosion phenomena. Corrosion Science 16, 111-118.

MARSH, G.P. & TAYLOR,. K.J. (1988): An assessment of carbon steel canisters for radioactive waste disposal. Corrosion Science 28, 289-320.

MATSUDA F., WADA R., FUJIWARA K. & FUJIWARA A. (1995): An evaluation of hydrogen evolution from corrosion of carbon steel in low/intermediate-level waste repositories. Mat. Res. Soc. Symp. Proc. 353, 719-726.

McGINNES D.F. (2002): Model radioactive waste inventory for reprocessing waste and spent fuel. Nagra Technical Report NTB 01-01, Nagra, Wettingen, Switzerland.

MORRISON S.J., METZLER D.R. & CARPENTER C.E. (2001): Uranium precipitation in a permeable reactive barrier by progressive irreversible dissolution of zerovalent iron. Environ. Sci. Technol. 35, 385-390.

MOYES L.N., JONES M.J., REED W.A., LIVENS F.R., CHARNOCK J.M., MOSSELMANS J.F.W., HENNIG C., VAUGHAN D.J. & PATTRICK R.A.D. (2002): An X-ray absorption spectroscopy study of Neptunium(V) reactions with mackinawite (FeS). Environ. Sci. Technol. 36, 179-183.

MOYES L.N., PARKMAN R.H., CHARNOCK J.M., VAUGHAN D.J., LIVENS F.R., HUGHES C.R. & BRAITHWAITE A. (2000): Uranium uptake from aqueous solution by interaction with goethite, lepidocrocite, muscovite and mackinawite: An X-ray absorption spectroscopy study. Environ. Sci. Technol. 34, 1062-1068.

MÜLLER-VONMOOS M. & KAHR G. (1983): Mineralogische Untersuchungen von Wyoming Bentonit MX-80 und Montigel, Nagra Technical Report NTB 83-12, Nagra, Wettingen, Switzerland.

MYNENI S.C.B., TOKUNAGA T.K. & BROWN G.E. (1997): Abiotic selenium redox transformations in the presence of Fe(II,III) oxides. Science 278, 1106-1109.

NAGRA (2002a): Project Opalinus Clay: Safety report. Demonstration of disposal feasibility for spent fuel, vitrified high-level waste and long-lived intermediate-level waste (Entsorgungsnachweis). Nagra Technical Report NTB 02-05, Wettingen, Switzerland.

NAGRA (2002b): Projekt Opalinuston - Synthese der geowissenschaftlichen Untersuchungsergebnisse. Entsorgungsnachweis für abgebrannte Brennelemente, verglaste hochaktive sowie langlebige mittelaktive Abfälle. Nagra Technical Report NTB 02-03, Nagra, Wettingen, Switzerland.

NAISH C.C., BALKWILL P.H., O'BRIEN T.M., TAYLOR K.J. & MARSH G.P. (1990): The anaerobic corrosion of carbon steel in concrete. NIREX Report NSS/R273, NIREX, United Kingdom.

NEALL F. (1994): Modelling of the near-field chemistry of the SMA repository at the Wellenberg site: application of the extended cement degradation model. Nagra Technical Report NTB 94-03, Nagra, Wettingen, Switzerland.

NERETNIEKS I. (1983): Approximate calculation of what happens with oxygen that is entrapped in the repository at the time of closure. In Corrosion resistance of a copper canister for spent nuclear fuel. The Swedish Corrosion Research Institute and its reference group. SKBF/KBS Technical Report 83-24, Appendix 4, pp. 39-45, SKBF, Stockholm, Sweden.

NOLD A.L. (2000): BE/HAA/LMA - Opalinuston. Zusammenstellung eingebauter Stahlmengen sowie deren Korrosionsoberflächen. Nagra Internal Report, Wettingen, Switzerland.

NORDSTROM D.K., PLUMMER L.N., LANGMUIR D., BUSENBERG E., MAY H.M., JONES B.F. & PARKHURST D.L. (1990): Revised chemical equilibrium data for major water-mineral reactions and their limitations. In D.C. Melchior & R.L. Bassett (eds.) Chemical Modeling of Aqueous Systems II., Washington D.C., American Chemical Society, ACS, Symposium Series 416, pp. 398-413.

NOVAKOVA A.A., GENDLER T.S., MANYUROVA N.D. & TURISHCHEVA R.A. (1997): A Mössbauer spectroscopy study of the corrosion products formed at an iron surface. Corrosion Science 39, 1585-1594.

PARKHURST D.L. & APPELO C.A.J. (1999): User's guide to PHREEQC (Version 2) - A computer program for speciation, batch reaction, one-dimensional transport, and inverse geochemical calculations. U.S. Geological Survey Water-Resources Investigations Report 99-4259, USA.

PEARSON J.F. (2002): Benken Reference Water Chemistry. Nagra Internal Report, Wettingen, Switzerland.

PEARSON J.F., SCHOLTIS A., GAUTSCHI A., BAEYENS B., BRADBURY M. & DEGUELDRE C. (1999): Chemistry of Porewater. In Mont Terri Rock Laboratory. Results of the hydrogeological, geochemical and geotechnical experiments performed in 1996 and 1997 (eds. M. Thury, P. Bossart). Landeshydrologie und -geologie, Geologische Berichte Nr. 23, pp. 129-146.

PEDERSEN K. (1997): Microbial life in granitic rock. FEMS Microbiology Reviews 20, 399-414.

PEDERSEN K. (2000): Microbial processes in radioactive waste disposal. SKB Technical Report TR-00-04, SKB, Stockholm, Sweden.

PEDERSEN K., MOTAMEDI M., KARNLAND O. & SANDÉN T. (2000): Mixing and sulphate-reducing activity of bacteria in swelling, compacted bentonite clay under high-level radioactive waste repository conditions. J. Appl. Microbiol. 89, 1038-1047.

PUIGDOMENECH I., AMBROSI J.-P., EISENLOHR L., LARTIGUE J.E., BANWART S.A., BATEMAN K., MILODOWSKI A.E., WEST J.M., GRIFFAULT L., GUSTAFSSON E., HAMA K., YOSHIDA H., KOTELNIKOVA S., PEDERSEN K., MICHAUD V., TROTIGNON L., RIVAS PEREZ J. & TULLBORG E.-L. (2001): O_2 depletion in granitic media. The REX project. SKB Technical Report TR-01-05, SKB, Stockholm, Sweden.

PUSCH R. (1999): Mobility and survival of sulphate-reducing bacteria in compacted and fully water saturated bentonite - microstructural aspects. SKB Technical Report TR-99-30, SKB, Stockholm, Sweden.

RÖLLIN S., SPAHIU K. & EKLUND U.-B. (2001): Determination of dissolution rates of spent fuel in carbonate solutions under different redox conditions with a flow-through experiment. J. Nucl. Mat. 297, 231-243.

SAROTT, F.-A., SPIELER, P. & PANDOLFO, P. (1995): Artificial ageing of hardened cement paste discs: compilation of experimental data records. Internal, not published document, Paul Scherrer Institute, Villigen, Switzerland.

SCHEIDEGGER A.M., GROLIMUND D., CUI D., DEVOY J., SPAHIU K., WERSIN P., BONHOURE I. & JANOUSCH M., (2003): Reduction of selenite on corroded iron surfaces: A micro-spectroscopic study. Journal de Physique IV (in press).

SCHWYN B., WERSIN P., BERNER U., WIELAND E. & NEALL F. (2003) Near-field chemistry of an ILW repository in Opalinus Clay. Nagra Internal Report, Wettingen, Switzerland.

SCOTT M.J. & MORGAN J.J. (1990): Energetics and conservative properties of redox systems. In: Chemical modeling of aqueous systems. D.C. Melchior & R.L. Bassett (eds.), American Chemical Society, Washington D.C. ACS Symposium Series 416, pp. 369-378.

SIMPSON J.P. (1984): Experiments on container materials for Swiss high-level waste disposal projects Part II. Nagra Technica Report NTB 84-01, Nagra, Wettingen, Switzerland.

SPAHIU K., WERME L. & EKLUND U.-B. (2000): The influence of near field hydrogen on actinide solubilities and spent fuel leaching. Radiochimica Acta 88, 507-511.

STROES-GASCOYNE S. (2002): Assessment of the likelihood of significant microbial activity in Opalinus Clay. Nagra Internal Report, Wettingen, Switzerland.

STROES-GASCOYNE S. & WEST J.M. (1997): Microbial studies in the Canadian nuclear fuel waste management program. FEMS Microbiology Reviews 20, 573-590.

STUCKI J.W. (1988): Structural iron in smectites. In Iron in Soils and Clay Minerals, J.W. Stucki, B.A. Goodman, U. Schwertmann (eds.), D. Reidel, Dordrecht, The Netherlands, pp. 625-675.

STUMM W. & MORGAN J.J. (1996): Aquatic Chemistry. 3rd edition, John Wiley & Sons, New York.

VOGT K. & KÖSTER H.M. (1978): Zur Mineralogie, Kristallchemie und Geochemie einiger Montmorillonite aus Bentoniten. Clay Minerals 13, 25-43.

WENK M. (1993): Wachstum mikrobieller Mischkulturen unter anaeroben alkalischen Bedingungen. Nagra Technical Report NTB 93-33, Nagra, Wettingen, Switzerland.

WERSIN P., SPAHIU K. & BRUNO J. (1994a): Time evolution of dissolved oxygen and redox conditions in a HLW repository. SKB Technical Report TR-94-02, Stockholm, Sweden.

WERSIN P., HOCHELLA M.F., PERSSON P., REDDEN G., LECKIE J.O. & HARRIS D.W. (1994b): Interaction between aqueous uranium(VI) and sulfide minerals: spectroscopic evidence for sorption and reduction. Geochim. Cosmochim. Acta 58, 2829-2843.

WEST J.M., McKINLEY I.G. & STROES-GASCOYNE S. (2002): Microbial effects on waste repository materials. In Interactions of microorganisms with radionuclides, M.J. Keith-Roach, F.R. Livens (eds.), Elsevier, pp. 255-277.

WINKLEHAUS C., DIGIANO F.A., WEBER W.J., MORGAN J.J. & BIRKNER F.B. (1966): Precipitation of iron in aerated ground waters. J. San. Eng. Divis. 92, 129-143.

APPENDIX A - Estimation of time scales for O_2 consumption

Case 1 - Partially Saturated Conditions with Uniform Corrosion

SF/HLW

The uniform corrosion rate of mild steel in aerated groundwater is 10 to 20 μm a^{-1} (MARSH & TAYLOR 1988). This rate is assumed here to be representative of the value in partially saturated bentonite. For the corrosion reaction

$$4Fe + 3O_2 + 2H_2O = 4FeOOH \quad \text{(A1)}$$

the oxygen consumption rate at the canister surface is :

$$\frac{3\,\text{mol}\,O_2}{4\,\text{mol}\,Fe} \times \frac{1.4\times10^{5}\ \text{mol}\,Fe}{\text{m}^3} \times \frac{2\times10^{-5}\ \text{m}}{\text{a}} = 2.1\,\text{mol}\,\text{m}^{-2}\,\text{a}^{-1} \quad \text{(A2)}$$

For the assumed initial O_2 inventory of 146 moles (chapter 1) and a spent fuel canister surface area of 18.2 m^2, the O_2 could be removed in

$$\frac{146\,\text{mol}}{18.2\,\text{m}^2 \times 2.1\,\text{mol}\,\text{m}^{-2}\,\text{a}^{-1}} = 3.8\,\text{a} \quad \text{(A3)}$$

if it were instantaneously transported to the canister surface. The effective diffusion coefficient of gas through unsaturated clay is a strong function of the degree of saturation (COLLIN & RASMUSON 1988). For example, for a decrease in the degree of saturation of bentonite from 100 to 90%, the diffusion coefficient increases by approximately three orders of magnitude, because of rapid diffusion in gas-filled pores. As a result, the reaction rate is not transport limited, and Eq. A3 gives a good rough estimate of the time involved for O_2 to be removed solely by canister corrosion.

ILW

Using the data from NOLD (2000) for the surface area of steel in the ILW-1 tunnel (23.5 m^2/ per metre of tunnel) and a corrosion rate of 0.1 μm/a, the rate at which the oxygen will be consumed can be calculated for the corrosion reaction according to Eq. A1. The oxygen consumption rate at the steel surface is:

$$\frac{3\,\text{mol}\,O_2}{4\,\text{mol}\,Fe} \times \frac{1.4\times10^{5}\ \text{mol}\,Fe}{\text{m}^3} \times \frac{1\times10^{-7}\ \text{m}}{\text{a}} = 0.01\,\text{mol}\,\text{m}^{-2}\,\text{a}^{-1} \quad \text{(A4)}$$

For the assumed initial O_2 inventory of 159 moles and a steel surface area of 23.5 m^2 per m of tunnel length, the O_2 could be consumed in

$$\frac{159\,\text{mol}}{23.5\,\text{m}^2 \times 0.01\,\text{mol}\,\text{m}^{-2}\,\text{a}^{-1}} = 676\,\text{a} \quad \text{(A5)}$$

For the ILW-2 tunnel that has about a three times smaller cross-section than that of ILW-1, an analogous calculations leads to the same O_2 depletion time.

Case 2 - Fully Saturated Bentonite with Uniform Corrosion

For the assumption of fully saturated bentonite, when O_2 diffusion is very slow, it can be inferred that the cathodic reaction is transport limited. It follows that the O_2 consumption by steel can be modelled assuming a c=0 boundary condition at the canister. A zero flux boundary condition can be assumed for oxygen transport into the bentonite from the surrounding rock. The solution to the diffusion equation within the bentonite for these boundary conditions is:

$$C = 4\frac{C_0}{\pi}\sum_{n=0}^{\infty}\left[\sin\left(\frac{\pi x}{2L}(2n+1)\right)\frac{1}{2n+1}\right]\exp\left[-\frac{D(2n+1)^2\pi^2 t}{4L^2}\right] \quad \text{(A6)}$$

where C and C_0 are the transient and initial concentrations of O_2 in the bentonite, L is the backfill thickness and D is the pore diffusion coefficient, assumed to be $5\text{x}10^{-10}$ m^2s^{-1} (NAGRA 2002a). At the outer edge of the bentonite ($x = L$), where the concentration will be highest,

$$\frac{C}{C_0} = \frac{4}{\pi}\sum_{n=0}^{\infty}\left[\frac{(-1)^n}{2n+1}\right]\exp\left[-\frac{D(2n+1)^2\pi^2 t}{4L^2}\right] \quad \text{(A7)}$$

Figure A1 shows that the oxygen concentration drops near to zero at the outer edge of the backfill within decades solely as a result of steel canister corrosion.

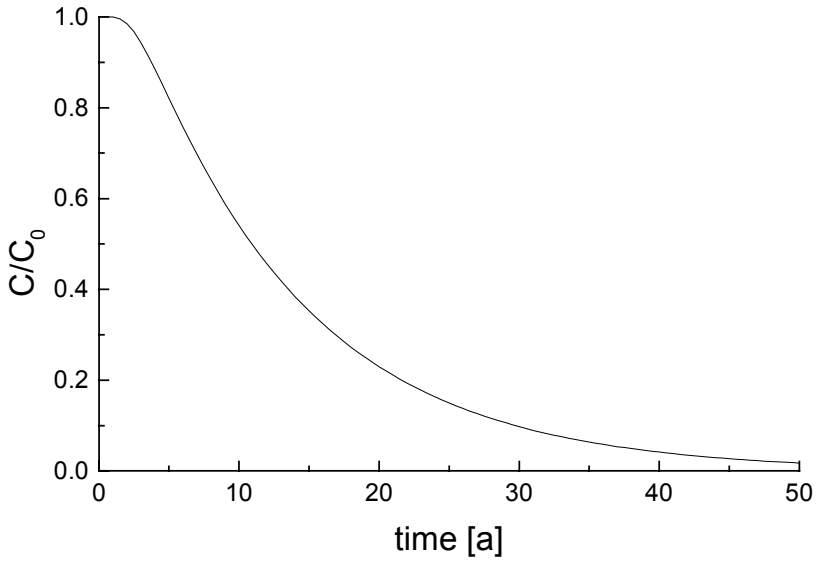

Figure A1: Relative oxygen concentration at the bentonite/host rock interface.

Calculated with Equation A7 for zero O_2 concentration at the canister/bentonite interface.

Case 3 Negligible Canister Corrosion with O_2 Reacting with Pyrite in the EDZ

A) SF/HLW

In this case O_2 will rapidly diffuse through high porosity dry bentonite and more slowly through the less porous oxidised part of the EDZ. It has been observed from mineralogical analysis of open tunnel systems of different ages in Opalinus Clay that the oxidation of pyrite occurs within the mm-range along the fracture network (MÄDER & MAZUREK 1998). The O_2 consumption rate is expected to be controlled by diffusion, since O_2-reaction with pyrite is fast (MÄDER & MAZUREK 1998; WERSIN et al. 1994a):

$$FeS_2 + {}^{15}/_4O_2 + {}^{7}/_2H_2O \text{ --> } Fe(OH)_3 + 2SO_4^{2-} + 4H^+ \qquad \text{(A8)}$$

The rate of depletion is estimated by assuming steady state diffusion across the oxidised rock around the repository tunnel. Hence, the consumption rate at the front (c = 0 boundary) is equal to rate of O_2 decrease from the inside of the repository. Also, this change of O_2 flux at steady state is equal to the flux across the oxidised rock. The solution of the diffusion equation under these boundary conditions is:

$$M_0 \ln(\frac{M}{M_0}) - M + M_0 = -4 \cdot \pi \cdot \varepsilon \cdot D \cdot \mathrm{X} \cdot t \qquad \text{(A9)}$$

where M_0 is initial mass and M the mass at time t of O_2 per m of tunnel (mol/m), ε is the porosity in the rock, D is the apparent diffusion coefficient of O_2 in the saturated rock and X is the amount of reductant times the stoichiometric factor per volume of rock (mol/m^3). The total amount of O_2 per canister is 146 moles (chapter 2). The tunnel length per canister (including EDZ) is 8.5 m, hence M_0 is equal to 17.18 mol/m. The porosity ε in the area of the EDZ is 0.15. X is obtained from the contents of pyrite in the rock (0.2 to 1.4%), the porosity and a stoichiometric factor of 3.75 (Eq. A8), giving a value of 150 - 751 mol/m^3 of rock. The apparent diffusion coefficient for non-sorbing dissolved species in Opalinus Clay is about $7 \cdot 10^{-11}$ m^2/s (NAGRA 2002b). In the area of the EDZ it will be at least a factor of 10 higher in view of expected unsaturated conditions at early stages of the repository. Because of uncertainties involved in pyrite concentrations and diffusion constants we derive time scales for a realistic case ($D = 7 \cdot 10^{-10}$ m^2/s, 1% pyrite) and pessimistic case ($D = 7 \cdot 10^{-11}$ m^2/s, 0.2% pyrite). Figure A2 illustrates the rates of oxygen consumption by applying Eq. A9 under the two conditions. The calculated time scales for O_2 depletion ($C/C_0 = 0.01$) is about 2 years for the realistic case and 100 years for the pessimistic case.

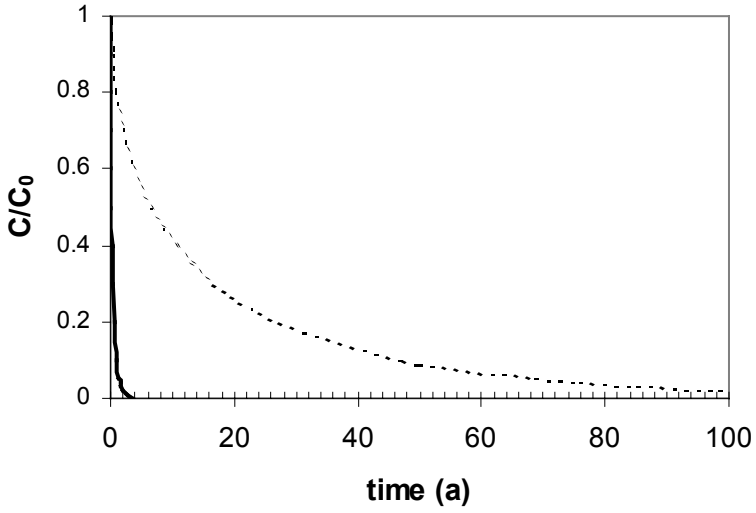

Figure A2: Relative oxygen concentration at the O_2 front in the host rock (SF/HLW case)

Calculated with Equation A9. Solid line: $D = 7 \cdot 10^{-10}$ m^2/s, 1% pyrite; dashed line: $D = 7 \cdot 10^{-11}$ m^2/s, 0.2% pyrite.

B) ILW

The treatment is analogue to the one for SF/HLW. For ILW-1 the initial O_2 is 160 mol per m of tunnel (Table 7.1). Applying Eq. A9 leads to time scales of O_2 depletion ($C/C_0 = 0.01$) of about 20 years for realistic case and to 950 years for the pessimistic case.

For ILW-2 the initial O_2 is 63 mol per m of tunnel (Table 7.1). Applying the same procedure as for ILW-1 leads to about 8 years for the realistic case and to 400 years for the pessimistic case.